Odorant receptors mediating avoidance of toxic mustard oils in *Drosophila melanogaster* are expanded in herbivorous relatives

Authors: Teruyuki Matsunaga[1*], Carolina E. Reisenman[2*], Benjamin Goldman-Huertas[3], Srivarsha Rajshekar[2], Hiromu C. Suzuki[2], David Tadres[4], Joshua Wong[5], Matthieu Louis[4], Santiago R. Ramírez[6], Noah K. Whiteman[2, 3*]

Affiliations:

[1] Department of Complexity Science and Engineering, Graduate School of Frontier Sciences, The University of Tokyo, Chiba, Japan

[2] Department of Molecular and Cell Biology, University of California Berkeley, Berkeley, CA

[3] Department of Integrative Biology, University of California Berkeley, Berkeley, CA

[4] Department of Molecular, Cellular, and Developmental Biology, University of California Santa Barbara, Santa Barbara, CA

[5] The Biochemistry, Cellular and Molecular Biology Graduate Program, The Johns Hopkins University School of Medicine

[6] Department of Evolution and Ecology, University of California Davis, Davis, CA

[*]Correspondence to: teru.matsu@edu.k.u-tokyo.ac.jp (T.M.), creisenman@berkeley.edu (C.E.R), and whiteman@berkeley.edu (N.K.W.)

KEY WORDS:

Drosophila melanogaster, olfaction, isothiocyanate, odorant receptor, Or42a, *Scaptomyza flava,* herbivory, evolution, Brassicales, mustard plants, AlphaFold2

ABBREVIATIONS:

AITC: allyl isothiocyanate

ITC: isothiocyanate

Or/OR: olfactory receptor

29 OSN: olfactory sensory neuron

30 Pb: palp basiconic

31 SSR: single sensillum recording

ABSTRACT:

Plants release defense volatile compounds that can deter herbivores. Among them are electrophilic toxins, such as isothiocyanates from mustard plants, that activate pain receptors by contact (i.e. taste) in many animals, including *Drosophila melanogaster*. While specialist insects have evolved strategies to tolerate toxicity and use mustard plants as hosts, it is unclear whether non-specialist insects detect and avoid electrophilic toxins via olfaction. To address this, and to understand if specialized insects co-opted these toxic compounds as hostplant olfactory cues, we leveraged closely related drosophilid species, including the microbe-feeding *D. melanogaster* and *Scaptomyza pallida*, and the mustard-feeding specialist *S. flava*. In olfactory assays, *D. melanogaster* exposed to allyl isothiocyanate volatiles were rapidly immobilized, demonstrating the high toxicity of this wasabi-derived compound to non-specialists. Through single sensillum electrophysiological recordings from olfactory organs and behavioral assays, we identified an Olfactory receptor (Or) necessary for volatile detection and behavioral aversion to allyl isothiocyanate in *D. melanogaster*. RNA sequencing and heterologous expression revealed that *S. flava* possess lineage-specific, triplicated homologs of this *Or,* and that each paralog exhibited broadened and distinct sensitivity to isothiocyanate compounds. Using AlphaFold2 modeling, site-directed mutagenesis and electrophysiological recordings, we identified two critical amino acid substitutions that changed the sensitivity of these paralogs from fruit-derived odors to isothiocyanates in the mustard specialist *S. flava*. Our findings show that non-specialists can detect electrophiles via olfaction, and that their olfactory systems can rapidly adapt to toxic hostplant niches through co-option and duplication of ancestral chemosensory genes with few amino acid changes.

1. INTRODUCTION:

Plants have evolved the ability to synthesize a diverse array of toxic specialized metabolites that can provide resistance against insect herbivory. In turn, herbivorous insects have evolved diverse morphological, physiological, and behavioral counter-strategies to avoid these chemicals if encountered, or to mitigate their effects if ingested (Mithöfer and Boland 2012). Some herbivores even co-opt these plant toxins as oviposition or feeding stimulants (and even as chemical defenses of their own). For instance, monarch butterfly larvae evolved insensitivity against cardenolides released from their milkweed host plants (Reichstein et al. 1968, Dobler et al. 2012). Many plant toxins are, however, far more promiscuous in their modes of action, which presents a different "evolutionary hurdle"

62 (Southwood 1972) to herbivores. Among them are various alkaloids, terpenoids, and electrophilic green
63 leaf volatiles (Noge and Becerra 2015; Yaffe et al. 2015; Iorio et al. 2022) that intoxicate and deter
64 herbivores by forming covalent bonds with biological molecules (War et al. 2012).

65 Mustard plants (Brassicales: Brassicaceae) such as thale cress (*Arabidopsis thaliana*), arugula
66 (*Eruca sativa*), and wasabi (*Eutrema japonicum*) have evolved a sophisticated chemical defense system
67 that produces electrophilic toxins (Ahuja et al. 2010). These plants produce non-toxic glucosinolates,
68 some of which are hydrolyzed *in planta* to form toxic electrophilic compounds such as isothiocyanates
69 (ITCs) (Hopkins et al. 2009). ITCs are reactive compounds defined by a −N=C=S functional group
70 attached to the rest of the molecule, wherein the electron-deficient carbon is attacked by nucleophiles.
71 Examples of ITCs include allyl ITC (AITC) derived from wasabi and radish *Raphanus sativus* (Cuellar-
72 Nuñez et al. 2022), and butyl ITC derived from the cabbage *Brassica oleracea* (MacLeod et al. 1989).
73 The chemical diversity of glucosinolates allows Brassicales plants to effectively deter a wide array of
74 herbivorous insects because different species have different mixtures of glucosinolates, making it more
75 difficult for insects to adapt (Winde and Wittstock 2011).

76 One herbivorous insect lineage that has evolved to cope with these toxic Brassicales metabolites
77 are obligated leaf-mining drosophilid flies in the genus *Scaptomyza* (e.g., *S. flava* and *S. montana*),
78 which is phylogenetically nested within the paraphyletic *Drosophila* subgenus. These *Scaptomyza*
79 mustard specialists, through rapid gene duplication and non-synonymous changes, have evolved some of
80 the most efficient ITC-detoxifying enzymes known from animals (Gloss et al. 2014, 2019).

81 While detoxification mechanisms help animals cope with at least some noxious compounds,
82 sensory detection and behavioral avoidance of these substances can act as a checkpoint to prevent
83 intoxication. Indeed, insects can behaviorally avoid toxic chemicals through gustation and/or olfaction
84 (e.g. Bernays and Chapman 1987; Stensmyr et al. 2012; Scott 2018; Chen and Dahanukar 2020; Dweck
85 and Carlson 2020). This includes avoidance of ITCs: exposure to volatile mustard plant extracts kills *D.*
86 *melanogaster* (Lichtenstein et al. 1964), and physical contact with AITC triggers repulsion via gustatory
87 receptor cells that express the nociceptive "wasabi receptor" TrpA1 and Painless (Al-Anzi et al. 2006;
88 Kang et al. 2010; Kim et al. 2010; Mandel et al. 2018). Additionally, volatile AITC causes behavioral
89 aversion in fire ants (*Solenopsis invicta*) (Hashimoto et al. 2019). However, the functional and genetic
90 basis underlying olfactory detection and avoidance of electrophilic toxins like ITC remain poorly
91 understood.

92 *Scaptomyza* species include both non-herbivorous (e.g., microbe-feeding) and herbivorous
93 species that use Brassicales plants (Aguilar et al. 2024). Herbivorous species have lost olfactory
94 receptors that ancestral microbe-feeding species (Whiteman et al. 2011, 2012; Peláez et al. 2023) like *D.*
95 *melanogaster* use to detect fermentation, microbial, and fruit odors (Goldman-Huertas et al. 2015).
96 Likely to aid hostplant location, the herbivorous specialist *S. flava* has evolved paralogous copies of the
97 Olfactory receptor 67b (which is expressed in antennal olfactory sensory neurons, OSNs) that respond to
98 ITCs. In contrast, the single copy of microbe-feeding *D. melanogaster* and *S. pallida* respond to green
99 leaf volatiles like *trans*-3-hexenol but not to ITCs (Matsunaga et al. 2021). Although these findings
100 provide insight into how sensory receptors evolved in specialists, how evolutionary changes facilitate
101 aversion and/or attraction to toxic compounds is still largely unknown, yet it is a central problem in
102 understanding how organisms invade toxic niches and herbivorous insects specialize on toxic host
103 plants.

104 In this study, we addressed the following three questions (Figure 1): (1) Do non-specialist insects
105 detect toxic volatile ITCs via olfaction and behaviorally avoid them? (2) Have the homolog olfactory
106 receptors of specialist insects evolved broader sensitivity to ITC hostplant compounds? (3) If so, what
107 molecular changes in these homologous olfactory receptors underlie this broadened sensitivity? To
108 address these questions, we first conducted behavioral toxicity assays and found that *D. melanogaster* is
109 rapidly immobilized by volatile exposure to AITC. We demonstrated that olfactory detection and
110 behavioral avoidance of this compound requires Olfactory receptor 42a (Or42a), which is expressed
111 specifically in maxillary palp OSNs (Ray et al. 2007). Next, in the specialist species *S. flava*, we
112 discovered that the *Or42a* paralog is triplicated and that the number of Or42a-positive OSNs is
113 expanded. Concomitantly, we found that these paralogous Or42a proteins are collectively sensitive to a
114 broad range of ITC compounds, whereas the single Or42a copies encoded in the genomes of the
115 microbe-feeding *S. pallida* and *D. melanogaster* respond only to AITC. Finally, AlphaFold2 3D
116 modeling, site-directed mutagenesis, and electrophysiological experiments identified two key amino
117 acid replacements that shifted the sensitivity of *S. flava* Or42a paralogs from fruit odors to ITCs.
118 Collectively, our findings demonstrate that plant-derived volatile toxins like ITCs negatively impact
119 non-specialists and are detected via olfaction to mediate avoidance, and that gene duplication events and
120 tuning shifts of olfactory receptors are coupled with specialization of herbivorous insects onto toxic
121 hostplants.

Figure 1

Q. 1

Can non-specialists detect volatile AITCs and behaviorally avoid them through olfaction?

> Figures 2, 3, and 4

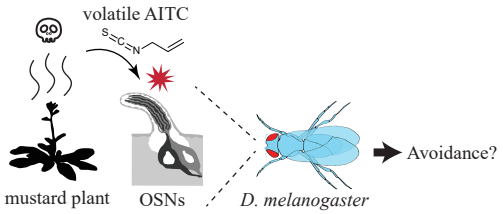

Q. 2

Have orthlogs from the mustard plant specialists evolved broaden sensitivity to hostplant ITC compounds?

> Figures 5, 6, and 7

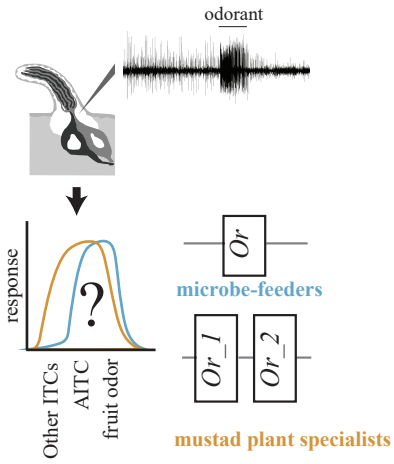

Q. 3

Which molecular changes in orthologs from specialists are important to reduce sensivitiy to fruit odors and to incrase sensitivity to hostplant odorants?

> Figure 8

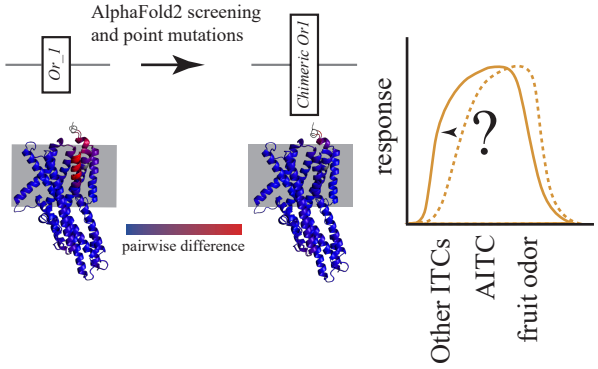

122

123 ## 2. RESULTS

124 ### 2-1. Volatile allyl isothiocyanate (AITC) rapidly immobilizes *D. melanogaster*

125 To assess the toxic effects of volatile AITC in *D. melanogaster*, we conducted immobility assays
126 with various concentrations of volatile AITC (from 1:500 to 1:2.5 vol/vol). In our experimental setup, a
127 fabric mesh separated the chamber containing the flies from the chamber containing the AITC solution
128 and therefore, flies were exposed to volatile AITC but could not contact (i.e. taste) the AITC solution
129 directly (Figure Supplement 1A). While all insects in both the control treatment and those exposed to
130 AITC 1:250 and 1:500 vol/vol remained active, most flies exposed to AITC concentrations ≥ 1:50
131 vol/vol became paralyzed (likely highly intoxicated or even dead) within 10 minutes (Figure 2). Thus,
132 this rapid immobilization indicates that plant-derived electrophilic compounds like AITC can have a
133 strong negative effect on flies, consistent with previous findings (Lichtenstein et al. 1964).

134

135 ### 2-2. Volatile AITC is detected by the maxillary palp olfactory receptor Or42a in *D. melanogaster*

136 The high toxicity caused by volatile AITC indicates that this volatile had the potential to be
137 detected by the fly's olfactory system, and that this could provide a fitness benefit if these volatile toxins
138 were then behaviorally avoided. We investigated this in *D. melanogaster* by conducting exhaustive
139 single sensillum recordings (SSR) from the fly's olfactory organs, the antennae and the maxillary palps,
140 upon stimulation with volatile AITC. Several olfactory sensory neurons (OSNs) showed excitatory
141 responses to AITC, but OSNs in palp basiconic sensilla 1a (pb1a) were the most activated (Figure 3A-B,
142 >100 spikes/sec). Because pb1a OSNs express Or42a (Couto et al. 2005), we investigated whether OSN
143 responses in this sensilla type are indeed mediated by this olfactory receptor. OSNs in pb1 sensilla from
144 genetic background control flies (*w1118*) showed strong responses to volatile AITC, while these OSNs
145 showed no response in *Or42a* -/- flies (Figure 3C, <2 spikes/second), indicating that Or42a detects
146 volatile AITC in these OSNs. Furthermore, OSNs in pb1a of $TrpA1^{1}$ null mutant flies responded
147 strongly to AITC (>150 spikes/second, Figure 3C), showing that the contact chemoreceptor TrpA1 is
148 not necessary for maxillary palp olfactory detection of this compound.

149

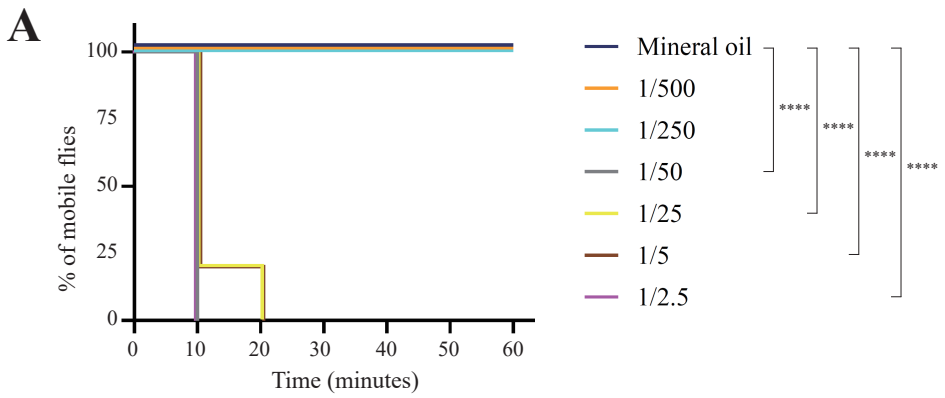
A
100
75
50
25
0
% of mobile flies
0
10
20
30
40
50
60
Time (minutes)
Mineral oil
1/500
1/250
1/50
1/25
1/5
1/2.5
****
****
****
****

Figure 2

Figure 3

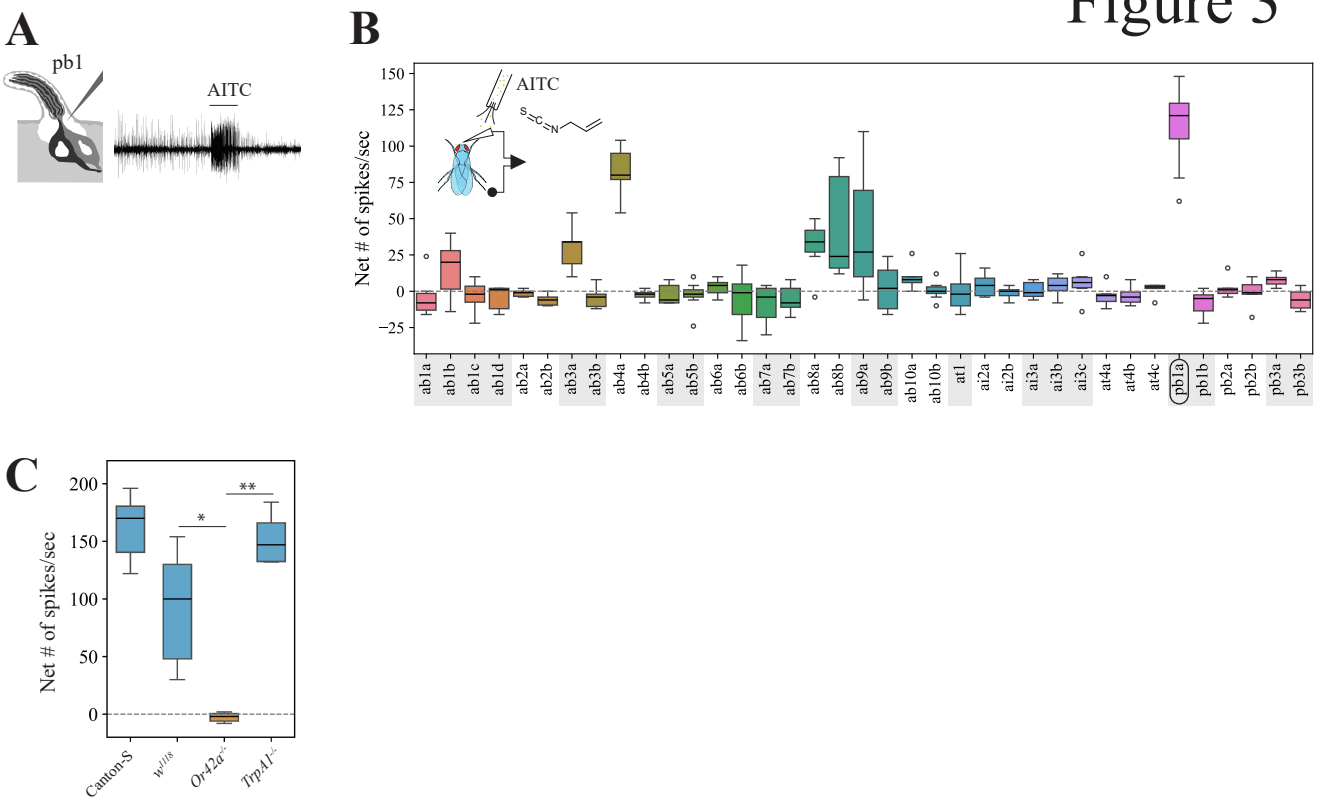
A
pb1
AITC
B
AITC
Net # of spikes/sec
150
125
100
75
50
25
0
−25
ab1a
ab1b
ab1c
ab1d
ab2a
ab2b
ab3a
ab3b
ab4a
ab4b
ab5a
ab5b
ab6a
ab6b
ab7a
ab7b
ab8a
ab8b
ab9a
ab9b
ab10a
ab10b
at1
ai2a
ai2b
ai3a
ai3b
ai3c
at4a
at4b
at4c
pb1a
pb1b
pb2a
pb2b
pb3a
pb3b
C
Net # of spikes/sec
200
150
100
50
0
*
**
Canton-S
w1118
Or42a-/-
TrpA1-/-

150 **2-3. Volatile allyl isothiocyanate repels *D. melanogaster* via the olfactory receptor Or42a**

151 Next, we examined if Or42a plays a role at the behavioral level. We conducted a positional
152 olfactory assay based on Ohashi and Sakai (2015) with modifications to prevent flies from physically
153 contacting the odor source. Female flies (n=10-12) were released in a dispositive consisting of two glass
154 tubes, each of which was connected to a vial containing an odor solution or a vial loaded with a solvent
155 (Figure Supplement 1B). The number of flies in each tube (hereafter "odorless/control tube" and
156 "odorous/test tube") as well as in the release section was counted every five minutes up to minute 35
157 (and again at 65 minutes). To validate this assay, we confirmed that wildtype *D. melanogaster* flies
158 (strain Canton-S) showed normal olfactory-guided behavior in this behavioral set-up using apple cider
159 vinegar (one-sample signed rank tests, $p<0.05$ in all cases, n=21, Supplementary File 4), a well-
160 established *D. melanogaster* olfactory attractant (Semmelhack and Wang 2009; Becher et al. 2010). We
161 then tested whether AITC causes olfactory repellence. For these and all forthcoming behavioral
162 experiments, we used as a genetic background control an "empty Gal4 control" line (line # 68384)
163 which carries *white* in the background of a *white* mutation, as in all the mutant fly lines. These control
164 flies and wild-type Canton-S flies avoided the AITC tube at various time points (25, 30, 35 and 65
165 minutes, Figure 4A and Figure Supplement 2A). In contrast, *Or42a-/-* mutants avoided the AITC tube
166 only at the 65 minutes time point (Figure 4A), possibly by taste detection of AITC via TrpA1 (volatile
167 AITC molecules might have adhered to the glass tube walls at this point). Importantly, we confirmed
168 that *Or42a-/-* mutants are capable of odor-mediated olfactory orientation in dual-choice trap assays
169 offering apple cider vinegar vs. water (described in Matsunaga et al., 2021): all captured flies were
170 recruited to the odor-baited trap (N=8 tests, n=20 females/test; Wilcoxon-matched pairs test, $p<0.005$;
171 Supplementary File 4). These results suggest that *Or42a* plays a crucial role in mediating olfactory-
172 driven behavioral aversion to AITC.

173 Given that detection of food-related volatiles is known to increase sugar consumption
174 (Reisenman and Scott, 2019), and that palp OSNs are located near the mouthparts, we reasoned that
175 volatile detection of toxic/aversive odors such as AITC would instead suppress sugar consumption. In
176 each test, we offered starved *D. melanogaster* (n=10-15 females/test) 50 mM glucose water solution
177 dyed blue for 15 minutes in presence or absence of an odor: one group of flies was exposed to volatile
178 AITC (1:500 vol/vol; flies could not contact the odor solution), and the control group was exposed to the
179 mineral oil solvent (Figure Supplement 1C; flies could not contact the odor source). We calculated a

Figure 4

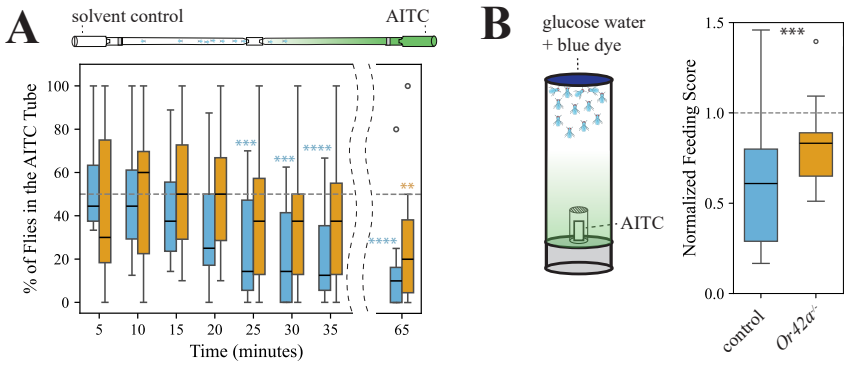
A
solvent control
AITC
% of Flies in the AITC Tube
100
80
60
40
20
0
***
***
****
****
**
5
10
15
20
25
30
35
65
Time (minutes)
B
glucose water
+ blue dye
AITC
Normalized Feeding Score
1.5
1.0
0.5
0.0
***
control
Or42a-/-

180 feeding score/test (each vial constitutes a biological replicate) based on the amount of blue dye in the
181 abdomen of flies. Control flies fed less when volatile AITC was present than in the presence of the
182 solvent (one-sample signed rank tests on normalized data, $p<0.001$; Figure 4B). *Or42a-/-* mutant flies
183 fed less in the presence of AITC volatiles as well ($p<0.05$), but their feeding scores were higher than
184 those of the control group ($p<0.001$, Mann-Whitney U test; Figure 4B). Altogether, these results show
185 that Or42a mediates aversion to AITC volatiles in two different behavioral contexts.

186 While we showed that Or42a-positive OSNs mediate behavioral aversion to AITC (Figure 4),
187 Dweck et al. (2016) found that these OSNs mediate attraction to some fruit/fermentation volatiles. We
188 thus tested whether Or42a also mediates behavioral attraction to such compounds in our experimental
189 set-up/s using γ-hexalactone, which has been reported to activate Or42a-positive OSNs (Dweck et al.,
190 2016). In the positional olfactory assay, genetic background control and wildtype Canton-S flies, but not
191 *Or42a-/-* mutants, were attracted γ-hexalactone 1:10 vol/vol at various time points (one-sample signed
192 rank tests, $p<0.05$ for both lines; Figure Supplement 2D and Supplementary File 4). Similarly, in
193 consumption assays, Canton-S flies increased their feeding in the presence of volatile γ-hexalactone 1:50
194 vol/vol, but this effect was lost in *Or42a-/-* mutants (Figure Supplement 2J). Additionally, we found that
195 volatile γ-hexalactone, contrary to what we observed in tests with AITC, does not immobilize flies
196 (Figure Supplement 2K). Thus, our behavioral assays show that volatile γ-hexalactone attracts *D.*
197 *melanogaster* via *Or42a* and is harmless, in line with previous results (Dweck et al., 2016).

198 Given that Or42a OSNs mediates both repellence to AITC and attraction to γ-hexalactone
199 (Figure 4 and Figure Supplement 2A-E, J), we hypothesized that additional OSNs contribute to mediate
200 these contrasting behavioral responses. We performed exhaustive SSR from antennae and maxillary
201 palps and found that pb1a OSNs were the only ones activated by γ-hexalactone among basiconic,
202 intermediate, and trichoid sensilla (Figure Supplement 2L). Due to technical limitations, we were unable
203 to study antennal coeloconic sensilla, but Oh et al. (2021) reported that this odor activates Or35a OSNs
204 in ac3b (Yao et al. 2005). In contrast, AITC activated several OSNs within the above mentioned sensilla
205 types, including Or7a OSNs (>75 spikes/second, Figure 3B), which are housed in ab4a (Lin et al. 2015).
206 Thus, we investigated whether *Or7a* and *Or35a* could respectively contribute to mediate the observed
207 behavioral repellence to AITC and attraction to γ-hexalactone. Compared to genetic background
208 controls, *Or7a -/-* flies showed less aversion to AITC in the positional olfactory assay (Figure
209 Supplement 2F-G), while *Or35a -/-* flies lost the attraction to γ-hexalactone (Figure Supplement 2H-I).

210 Thus, not only Or42a, but Or35a and Or7a are also necessary to mediate attraction/repellence behaviors
211 to these odorants: activation of both Or42a and Or7a OSNs by AITC might mediate aversion, while
212 activation of both Or42a and Or35a OSNs by γ-hexalactone might mediate attraction. Our findings thus
213 support a combinatorial hypothesis of odor coding with respect to these ligands, and indicate that the
214 valence of Or42a-mediated behavioral responses is context-dependent (Figure Supplement 2M).

215

216 **2-4. Pb1a-like OSNs in Brassicales-specialists evolved broadened sensitivity to isothiocyanates**

217 We next investigated how the evolutionary transitions from microbe-feeding to herbivory have
218 affected the odor tuning of OSNs, using the reference species *D. melanogaster* as well as species within
219 *Scaptomyza*: the microbe-feeding *S. hsui* and *S. pallida*, and the herbivorous Brassicales specialists *S.*
220 *flava* and *S. montana* (Kim et al. 2021; Peláez et al. 2023). We investigated whether *Scaptomyza* species
221 have pb1-like sensilla homologous to *D. melanogaster* pb1 and if so, the extent to which they respond to
222 a broader range of ITC compounds, since Brassicales plants release many different ITCs upon wounding
223 (MacLeod et al. 1989; Cuellar-Nuñez et al. 2022).
224 We first validated our methods for functional characterization of sensilla. Using compounds that
225 serve as diagnostic for the three sensilla types found in the maxillary palps of *D. melanogaster* (see
226 methods for details), various other plant-derived volatiles and several Brassicales-derived ITCs, we
227 confirmed the presence of three different types of palp sensilla (pb1, pb2 and pb3) in this species (Figure
228 5 and Figure Supplements 3-4). As we observed before, *D. melanogaster* pb1a OSNs responded to
229 AITC (>120 spikes/sec), but not to the other ITCs tested (<10 spikes/sec, Figure 5). We next
230 characterized OSNs in pb sensilla in the four *Scaptomyza* species and used the spike rate to determine if
231 data clustered by sensilla type (Figure 5, Figure Supplement 3-4). In all *Scaptomyza* species sensilla fell
232 into three functional classes, two of which were functionally similar to *D. melanogaster* pb1 and pb2
233 (we termed them pb1-like and pb2-like). The third class was functionally different to any *D.*
234 *melanogaster* palp sensilla type and clustered separately (termed pb3-like, Figure Supplement 3-4). As
235 in *D. melanogaster*, AITC activated pb1a-like sensilla in all four *Scaptomyza* species (Figure 5) but
236 several other ITCs, including isobutyl ITC, butyl ITC, and *sec*-butyl ITC, additionally activated *S. flava*
237 and *S. montana* pb1a-like OSNs (Figure 5).

238 We also conducted dose-responses to various odorants from pb1a/pb1a-like sensilla of the
239 microbe-feeding species (*D. melanogaster, S. hsui* and *S. pallida*) and the Brassicales specialists (*S.*

Figure 5

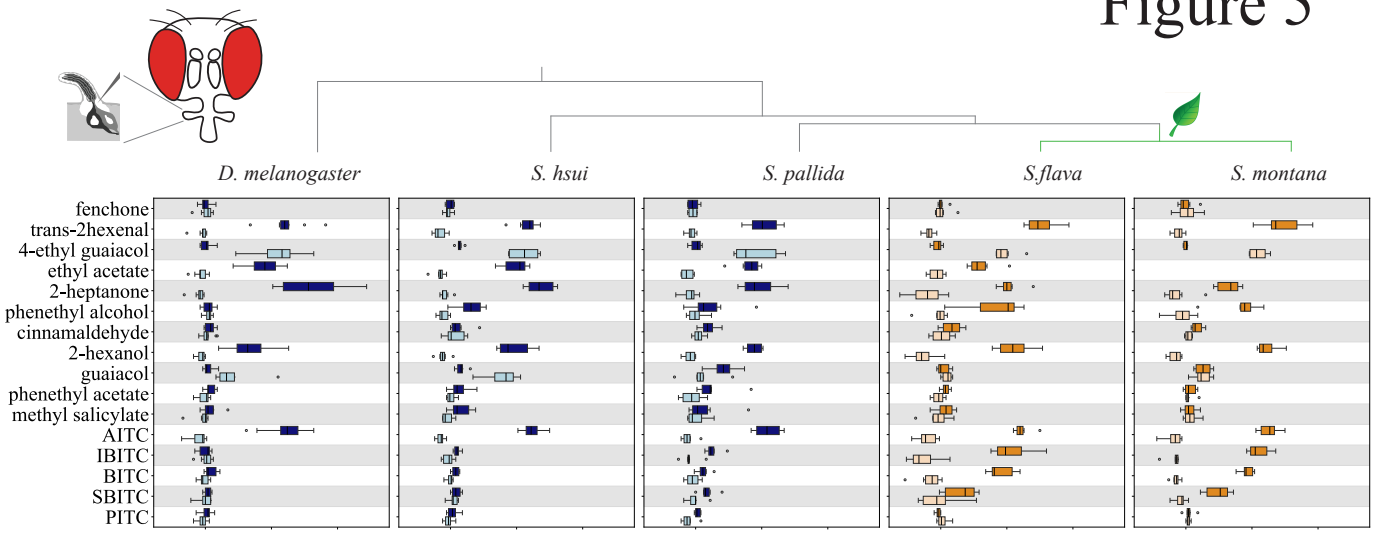
D. melanogaster
S. hsui
S. pallida
S.flava
S. montana
fenchone
trans-2hexenal
4-ethyl guaiacol
ethyl acetate
2-heptanone
phenethyl alcohol
cinnamaldehyde
2-hexanol
guaiacol
phenethyl acetate
methyl salicylate
AITC
IBITC
BITC
SBITC
PITC

240 *flava* and *S. montana*). For the most part, responses increased with increasing odorant concentration
241 (Figure Supplement 5A). For comparing odor sensitivity across species, we calculated the odorant
242 concentration required to elicit a biological response halfway between the baseline and the maximum
243 (50% effective concentration, EC_{50}; Figure Supplement 5D). In agreement with its herbivore habit, the
244 EC_{50} for the fruit odor γ-hexalactone was higher in the herbivore *S. flava* than in the microbe-feeding *S.*
245 *hsui* (*S. flava* had even lower sensitivity to this odorant than the herbivore *S. montana*; Figure
246 Supplement 5B and D). The EC_{50} for *trans*-hexenal was lower in the two herbivores species than in *D.*
247 *melanogaster* or *S. hsui* (Figure Supplement 5D), and *S. flava* was even more sensitive to this odorant
248 than *S. montana* (Figure Supplement 5C). Similarly, the EC_{50} for AITC was lower in all the *Scaptomyza*
249 species, but the two mustard specialists had similar EC_{50} for all the ITCs tested (Figure Supplement 5D,
250 right). Overall, all these findings suggest that microbe-feeding species exhibit higher sensitivity to the
251 fruit odor γ-hexalactone, whereas Brassicales specialists show heightened sensitivity to electrophilic
252 *trans*-2-hexenal and ITCs.

253

254 **2-5. *Or42a* is triplicated in the genome of *S. flava* and is highly expressed in the maxillary palps**

255 Genomic analysis across the *Scaptomyza* genus revealed a duplication of *Or42a* in the lineage
256 leading to all known *Scaptomyza*, while the *D. melanogaster* outgroup had a single *Or42a* homolog
257 (Figure Supplement 6A). Notably, syntenic analysis indicated that *S. flava* has a species-specific tandem
258 triplication in one of the *Or42a* duplicates, resulting in three tandem paralogs, which we named *Or42a2*,
259 *Or42a3*, and *Or42a4* (Figure 6A and Figure Supplement 6A-B). In contrast, *S. montana*, *S. graminum,*
260 *S. pallida* and *S. hsui* retained only two *Or42a* paralogs.

261 Given these differences in the Or42a gene copy number across species, we conducted species-
262 and sex-specific RNA transcriptome analyses of OSNs in the maxillary palps of the microbe-feeding *S.*
263 *pallida* and the mustard plant specialist *S. flava*. We confirmed the expression of *S. pallida Or42a* and *S.*
264 *flava Or42a2-4* in these organs (Figure 6B; Figure Supplement 7). Interestingly, the *S. flava Or42a*
265 paralogs were each expressed at levels comparable to those of other *Or* genes, such as *Or33c*, the
266 homolog of which is expressed in pb2a OSNs in *D. melanogaster* (Figure Supplement 7). We found that
267 *S. pallida Or42a2* and *S. flava Or42a2-4* were expressed in the respective maxillary palp of each
268 species, whereas *S. pallida Or42a1* and *S. flava Or42a1* were not expressed (Figure 6B).

269

Figure 6

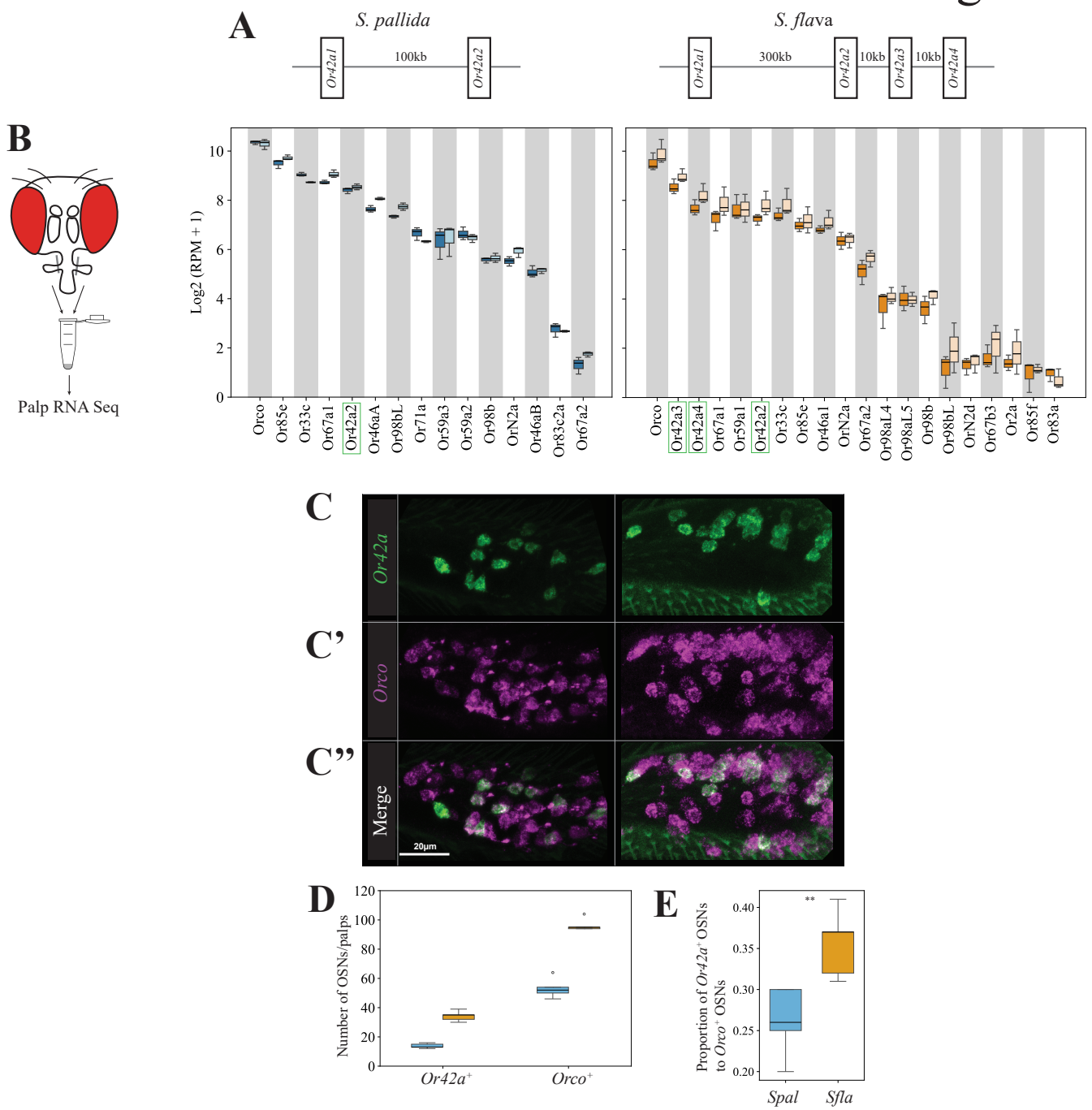
A
S. pallida
Or42a1
100kb
Or42a2
S. flava
Or42a1
300kb
Or42a2
10kb
Or42a3
10kb
Or42a4
B
Palp RNA Seq
Log2 (RPM + 1)
Orco
Or85e
Or33c
Or67a1
Or42a2
Or46aA
Or98bL
Or71a
Or59a3
Or59a2
Or98b
OrN2a
Or46aB
Or83c2a
Or67a2
Or42a3
Or42a4
Or59a1
Or33c
Or85e
Or46a1
OrN2a
Or67a2
Or98aL4
Or98aL5
Or98b
Or98bL
OrN2d
Or67b3
Or2a
Or85f
Or83a
C
C'
C''
Or42a
Orco
Merge
20μm
D
Number of OSNs/palps
Or42a+
Orco+
E
Proportion of Or42a+ OSNs to Orco+ OSNs
**
Spal
Sfla

270 **2-6. The Brassicales specialist *S. flava* has more *Or42a*-positive olfactory sensory neurons.**

271 Given that pb1a-like OSNs likely express *Or42a* (Figure 6B), we hypothesized that the number
272 of *Or42a*-positive OSNs is higher in the specialist species. To test this, we quantified the number of
273 *Or42a*-positive OSNs in *S. flava* and *S. pallida* using hybridization chain reaction RNA fluorescent in
274 situ hybridization (RNA FISH). We designed a *S. flava Or42a* RNA probe based on the conserved
275 sequence region of *S. flava Or42a2*, *3*, and *4*, as the high sequence similarity among these paralogs
276 prevented the design of paralog-specific probes. We found that the maxillary palps of *S. flava* contained
277 more *Or42a*-positive OSNs and more *Orco*-positive OSNs (Orco is a highly conserved co-receptor
278 necessary for odorant receptor olfactory function, Larsson et al., 2004) than those of *S. pallida* (Figure
279 6C-D). Because all maxillary palp OSNs express Orco (Larsson et al. 2004), the number of Orco-
280 positive OSNs represents the total number of palp OSNs. Importantly, the ratio of the total number of
281 *Or42a*-positive OSNs to the total number of *Orco*-positive OSNs was higher in *S. flava* (Figure 6E).
282 These results indicate that *S. flava* has not only more *Or42a*-positive OSNs in the maxillary palps, but
283 also a greater proportion of *Or42a*-positive OSNs relative to the overall number of OSNs. Accordingly,
284 we predicted that the number of pb1-like sensilla would be also overrepresented in mustard specialists.
285 To test this, we generated functional anatomical maps of sensilla on the anterior part of the maxillary
286 palps of the *Scaptomyza* species (and of *D. melanogaster* for comparison) using diagnostic chemicals
287 (Figure Supplement 8-9, Supplementary file 10). While *D. melanogaster* had a relatively randomized
288 distribution of sensilla on the palps, consistent with previous reports (de Bruyne et al. 1999), all four
289 *Scaptomyza* species exhibited a more organized sensilla pattern, with pb1-like, pb2-like, and pb3-like
290 respectively located medially, distally, and proximally, as reported in *D. mojavensis*, which is more
291 closely related to all *Scaptomyza* spp. than *D. melanogaster* (Crowley-Gall et al. 2016). We then
292 quantified the number of each sensilla type across species and found that both *S. flava* and *S. montana*
293 have a larger number of pb1-like than of pb2-like or pb3-like sensilla, while *D. melanogaster* and the
294 other two microbe-feeding *Scaptomyza* species had similar proportions of each sensilla type (Figure
295 Supplement 8-9). These findings, showing a triplication of Or42a, along with an expansion in the
296 number of Or42a-positive OSNs and pb1a-like sensilla, are in line with the enhanced capacity of
297 Brassicales-specialist *Scaptomyza* species to detect volatile ITCs.

298

299 **2-7. Paralog-specific functional evolution of the olfactory receptor Or42a.**

300 We next investigated whether the increased sensitivity of *S. flava* pb1a-like OSNs to ITCs
301 (Figure 5) also resulted from changes in the odor tuning of the Or42a triplicates. To test this, we
302 expressed *D. melanogaster* Or42a, *S. pallida* Or42a2, and *S. flava* Or42a2-4 in *D. melanogaster*
303 antennal trichoid 1 (at1) OSNs (in the background of a null mutation for *Or67d*, the at1 cognate receptor
304 Kurtovic et al. 2007) and conducted functional analysis. We found that γ-hexalactone, *trans*-2-hexenal,
305 and AITC strongly activated OSNs expressing *D. melanogaster* Or42a (>79 spikes/second) or *S. pallida*
306 Or42a2 (>96 spikes/sec), while the other ITC compounds evoked much weaker responses from these
307 two orthologs (respectively <11 and 18 spikes/second; Figure 7A-B). OSNs expressing *S. flava* Or42a3
308 or *S. flava* Or42a4 were also very sensitive to AITC and *trans*-2-hexenal but additionally responded to
309 isobutyl ITC and butyl ITC (> 87 and 46 spikes/second, respectively; Figure 7B), consistently with the
310 odor response profiles of *S. flava* pb1a OSNs (Figure 5). Notably, OSNs expressing *S. flava* Or42a4
311 showed only small responses to γ-hexalactone (<10 spikes/second), and *S. flava* Or42a2 was only
312 activated by AITC (Figure 7B). These results are in line with the broader ITC sensitivity of *S. flava* pb1a
313 OSNs compared to that of *D. melanogaster* pb1a and *S. pallida* pb1a-like OSNs. Altogether, our
314 findings reveal paralog-specific functional evolution of Or42a triplicates in *S. flava*, wherein different
315 paralogs evolved distinct sensitivities to different ITCs and fruit odors.

316

317 **2-8. AlphaFold2-led screening with ectopic expression of *S. flava* Or42a reveals the molecular**
318 **changes underlying changes in odor sensitivity**

319 We next investigated which amino acid substitutions in *S. flava* O42a4 may have led to the gain
320 of sensitivity to butyl ITC and the decreased sensitivity to γ-hexalactone (there are 32 amino acid
321 differences between *S. flava* Or42a3 and *S. flava* Or42a4, Figure Supplement 10A). To explore the
322 structural basis of these functional differences, we predicted the 3D structures of *S. flava* Or42a3 and *S.*
323 *flava* Or42a4 and aligned the resulting models in 3D space using PyMol (Jumper et al. 2021; Mirdita et
324 al. 2022; Benton and Himmel 2023; Himmel et al. 2023).

325 We first confirmed that the predicted local distance difference test scores for the *S. flava* Or42a3
326 and *S. flava* Or42a4 structures were sufficiently high to ensure confidence in the 3D predictions, except
327 for the N-terminal and C-terminal regions (Figure Supplement 10B). The most striking 3D structure

Figure 7

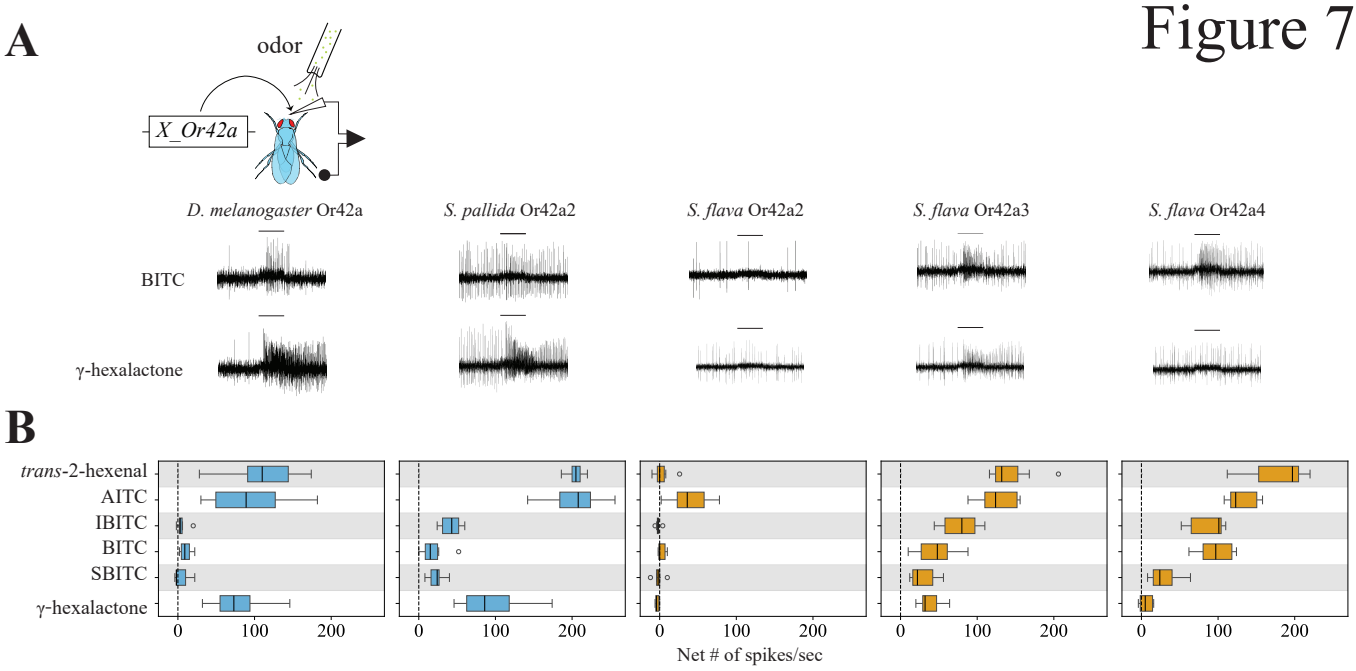
A
odor
X_Or42a
D. melanogaster Or42a
S. pallida Or42a2
S. flava Or42a2
S. flava Or42a3
S. flava Or42a4
BITC
γ-hexalactone
B
trans-2-hexenal
AITC
IBITC
BITC
SBITC
γ-hexalactone
0
100
200
Net # of spikes/sec

difference between *S. flava* Or42a3 and *S. flava* Or42a4 was in the S5 and S6 helices in the transmembrane region (~1.7Å root mean square deviation, Figure 8A-A' and Figure Supplement 11A-C), which is reported to contain the ligand binding pockets of Ors (Del Mármol et al. 2021; Wang et al. 2024; Zhao et al. 2024). We then substituted each of the 32 amino acids in *S. flava Or42a4* individually with the corresponding residues from *S. flava* Or42a3 *in silico,* predicted the 3D structures of the chimeras, and aligned them with *S. flava* Or42a4 in 3D space until the local structural differences were resolved. Remarkably, the substitutions of A181D and S307P in *S. flava* Or42a3 (hereafter referred to as A181D S307P) reduced the root mean square deviation to approximately 0.1 Å in the S5 and S6 helices when aligned with *S. flava* Or42a4, indicating that these two mutations are likely to explain the local structural differences (Figure 8A-A' and Figure Supplement 11A-C).

We then used the *D. melanogaster* at1 empty neuron system to investigate whether these two amino acid substitutions could account for the differences in odor sensitivity between *S. flava* Or42a4 and *S. flava* Or42a3. The A181DS307P variant and the two *S. flava* paralogs showed similar moderate responses to butyl ITC (Figure 8B-C). However, the butyl ITC to γ-hexalactone response ratios of *S. flava* Or42a4 and A181D S307P were not different from each other, but were both higher than the response ratio of *S. flava* Or42a3 (Figure 8D). These findings suggest that the two amino acid substitutions in *S. flava* Or42a4 are sufficient to increase the sensitivity to butyl ITC relative to γ-hexalactone. This effect was observed in flies carrying the heterozygous genotype A181D S307P/+ but not in flies with the homozygous A181D S307P genotype (Compare Figure 8C-D with Figure Supplement 12), possibly due to response saturation or dominant-negative effects. In summary, our findings demonstrate that the A181D and S307P substitutions in *S. flava* Or42a4 are critical for shifting the receptor's sensitivity from fruit odorants to ITCs.

3. DISCUSSION

In this study we addressed three major questions: (1) Do non-specialist insects use olfaction to detect and avoid toxic isothiocyanate (ITC) compounds released by mustard plants? (2) Was this ancestral olfactory capability co-opted and expanded in mustard plant specialists for facilitating hostplant detection? (3) What molecular changes underlie the olfactory receptor sensitivity shift from fruit odors to hostplant-derived toxins? Answering these questions is important for understanding which molecular changes in the chemoreceptors of ancestral non-specialists enabled adaptation to toxic ecological niches

Figure 8

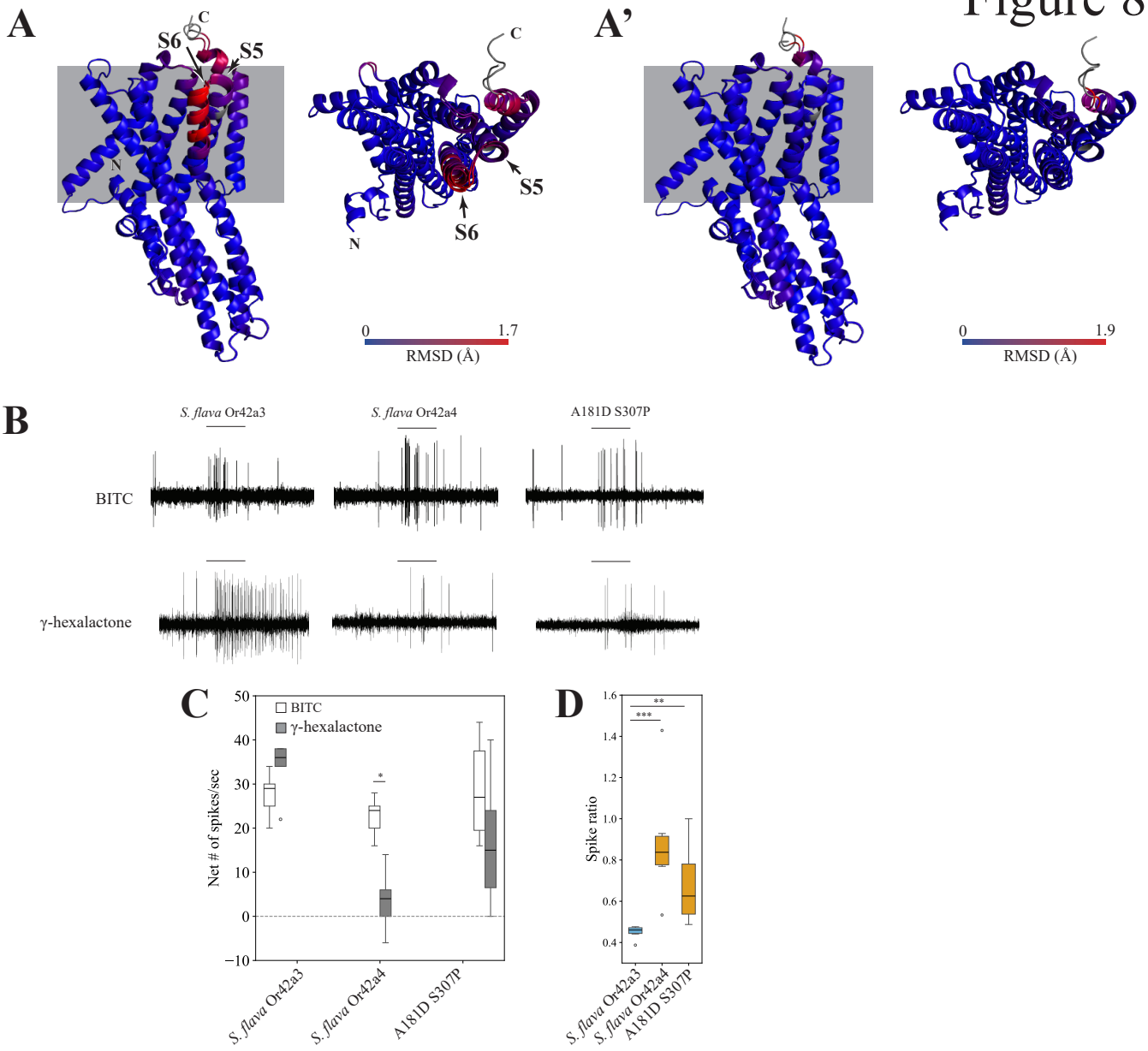
A
S6
C
S5
N
C
S5
S6
N
0
1.7
RMSD (Å)
A'
0
1.9
RMSD (Å)
B
S. flava Or42a3
S. flava Or42a4
A181D S307P
BITC
γ-hexalactone
C
BITC
γ-hexalactone
Net # of spikes/sec
50
40
30
20
10
0
−10
*
S. flava Or42a3
S. flava Or42a4
A181D S307P
D
Spike ratio
1.6
1.4
1.2
1.0
0.8
0.6
0.4
**
***
S. flava Or42a3
S. flava Or42a4
A181D S307P

358 in derived species, a central issue in the evolution of herbivory. We found that plant-derived ITCs are
359 detrimental to microbe-feeding *D. melanogaster* through volatile exposure, and that the olfactory
360 receptor Or42a is necessary for its detection and for behavioral aversion. To our knowledge, this is the
361 first ITC-olfactory detector in *D. melanogaster*. In the mustard plant specialist *S. flava*, homologous
362 olfactory receptors are triplicated and have an expanded ITC-sensitivity range, accompanied by an
363 increase in the number of ITC-detecting OSNs. Finally, we discovered that two amino acid changes are
364 sufficient to shift the odor sensitivity of these paralogs from fruit odors to ITC volatiles.
365

366 **3-1. The plant-derived volatile allyl isothiocyanate is toxic to *D. melanogaster* and its detection and**
367 **avoidance is mediated by *Or42a*-positive olfactory sensory neurons**

368 Plants have evolved a diverse array of specialized metabolites, including electrophilic ITCs, that
369 repel or intoxicate insects (Ibanez et al. 2012; Noge and Becerra 2015; Tocmo et al. 2021). ITCs are not
370 only detected by contact (Bell et al. 2018), but some mustard-plant specialists such as the diamondback
371 moth *Plutella xylostella* (Liu et al. 2020) and *S. flava* (Matsunaga et al. 2021) also detect these
372 compounds via olfaction. However, it was unclear whether non-specialists such as *D. melanogaster* have
373 evolved strategies to detect these toxic compounds using olfaction. We found that the olfactory receptor
374 Or42a is necessary for OSN responses in the sensilla where it is expressed (palp basiconic 1a sensilla,
375 Figure 3C). Furthermore, this Or was necessary for inducing olfactory aversion to AITC in two different
376 behavioral contexts (Figure 4 and Figure Supplement 2A). Thus, in *D. melanogaster*, Or42a works in
377 combination with the "wasabi" taste receptor" TrpA1 and Painless (Al-Anzi et al. 2006; Kang et al.
378 2010; Mandel et al. 2018), and possibly with other Ors (see next paragraph), to facilitate adaptive
379 behavioral avoidance of these chemicals. It remains to be tested whether other non-specialist organisms
380 across phyla also possess olfactory sensors tuned to volatile isothiocyanates.

381 We found that Or42a is also necessary for behavioral attraction to the fruit-derived volatile γ-
382 hexalactone (Figure Supplement 2D-E and J). How does a single olfactory channel mediate aversion to
383 AITC while also driving attraction to γ-hexalactone? Our experiments suggest that simultaneous
384 activation of Or42a and the "generalist" OR7a (which is housed in OSNs in ab4 and respond to aversive
385 odorants, Lin et al., 2015) could mediate aversion to AITC (Figure 4 and Figure Supplement 2F-G, M).
386 Similarly, simultaneous activation of Or42a and Or35a (which is housed in ac3b, responds to γ-
387 hexalactone and mediates attraction to yeast odors, Yao et al., 2005; Oh et al., 2021) could mediate

388 attraction to γ-hexalactone (Figure Supplement 2H-I, M). Future investigations at the circuit level,
389 particularly on the role of interglomerular interactions via local neurons in the insect primary olfactory
390 center (Haverkamp et al. 2018), should further elucidate the neural mechanisms mediating these
391 behavioral responses of opposite valence.

392

393 **3-2. Duplication and functional evolution of the olfactory receptors *Or42a* and *Or67b* in**
394 ***Scaptomyza* mustard plant specialists**

395 Brassicales specialist need to detect a wide range of ITC compounds for effective host plant
396 location, as these plants release species-specific volatile ITCs at particular ratios and concentrations (Wu
397 et al. 2021). We previously reported that *S. flava* also has triplicated and positively selected *Or67b*
398 copies (Matsunaga et al. 2021). The Ors encoded by these paralogous *Or67b* copies respond to aromatic
399 and some aliphatic ITCs in a paralog-specific manner, while the *D. melanogaster* and *S. pallida* Or67b
400 single copies did not respond to any volatile ITC compound (Matsunaga et al. 2021). However, all three
401 *S. flava* Or67b paralogs showed poor responses to organosulfur ITCs, including AITC. In this study, we
402 found that *S. flava* also expresses tandem triplicates of the *Or42a*s (*Or42a2*, *Or42a3*, and *Or42a4*;
403 Figure 6A and Figure Supplement 6). Furthermore, OSNs housed in the pb1a-like sensilla of the
404 mustard specialist species responded to many volatile ITCs, including AITC (Figure 5 and Figure
405 Supplement 5). Thus, the gene duplications and amino acid substitutions of Or42a, along with those of
406 Or67b, both likely play an important role in enabling Brassicales-plant specialist *Scaptomyza* species to
407 detect a wide range of ITCs. Furthermore, mustard plant specialization is likely aided by the losses of
408 genes encoding four olfactory receptors that detect fermentation odors in *D. melanogaster* and are
409 necessary for attraction to these odors, and by the loss of an ancestral olfactory receptor (*Or7a*, housed
410 in ab4a) that mediates aversion to AITC (Figure Supplement 2F-G; Goldman-Huertas et al. 2015).

411 What is the functional relevance of ITC-sensitive Ors expressed in two different olfactory
412 organs? Or67b in *S. flava* is primarily expressed in the antennae (Matsunaga et al. 2021), whereas Or42a
413 in *S. flava* and the other drosophilids is expressed in the maxillary palps (Figure 6B). In *D.*
414 *melanogaster*, maxillary palps OSNs have lower sensitivity thresholds to certain host-related compounds
415 compared to antennal OSNs (Dweck et al. 2016). Indeed, *S. flava* Or42a paralogs are much more
416 sensitive to AITC than the Or67b paralogs (compare Figure 5 with Figure 4 in Matsunaga et al. 2021).
417 Odor response redundancy between antennal and maxillary palp Ors could have evolved to further

underpin olfactory orientation over both long and short distances in drosophilids (Dweck et al. 2016). Given the proximity of Or42a OSNs to the mouthparts, their activation could potentially modulate feeding behaviors, as suggested in *D. melanogaster* (Shiraiwa 2008). *S. flava* and *S. montana* females feed on the juice that seeps into the leaf wounds they create in Brassicales plants before oviposition (Peláez et al. 2022). Given this stereotyped feeding behavior, while the activation of contact chemoreceptors by ITCs could help females assess the suitability of an oviposition site through taste, flies may also be aided by maxillary palp olfactory activation even before tasting the plants.

Although the OSNs in pb1a sensilla of the two mustard specialist species have a broad ITC response range (Figure 5), *S. flava* has triplicated *Or42a*s but *S. montana* has only one copy (Figure Supplement 6). This suggests that both the mustard plant specialization and the mutations underlying the expanded ITC sensitivity range of Or42a preceded the triplication of *Or42a*. What is then the adaptive value of the *Or42a* triplication? We observed that *S. flava* pb1a OSNs, which express at least one of the three triplicated Or42as (Figure 6A-B), exhibited reduced sensitivity to fruit-borne γ-hexalactone in comparison with *S. montana* pb1a OSNs (Figure Supplement 5). Only *S. flava* Or42a4 acquired the two key mutations that increased the ITC to γ-hexalactone response ratio, as evidenced by the weaker γ-hexalactone response of the chimeric Or compared to that of *S. flava* Or42a3 (Figure 8). In agreement with these observations, structural alignment of the 3D models predicted by AlphaFold2 revealed that *S. montana* Or42a2 aligned well with *S. flava* Or42a3, but not with *S. flava* Or42a4 (Figure Supplement 11D). Based on these findings, we hypothesized the following sequence in the evolution of Or42a (Figure Supplement 13): (1) mustard specialization and broadening of ITC sensitivity in the ancestral drosophilid Or42a that was already sensitive to some ITCs like AITC; (2) speciation and triplication of Or42a in *S. flava* but not in *S. montana*; (3) relaxation of evolutionary constraints due to gene duplications, allowing *S. flava* Or42a4 to reduce its sensitivity to γ-hexalactone. It was suggested that *S. flava* has a broader host range (Maca 1972, Martin 2004) than *S. montana*, which requires indolic glucosinolates to use plants as hosts (Gloss et al. 2017). Thus, although mustard specialization preceded the Or42a duplication, we hypothesize that gene duplication was an important event in driving adaptation to new ecological niches in herbivorous *Scaptomyza*.

445 **3-3. Evolution of specialized olfactory receptors is coupled with expansion of maxillary palp**
446 **sensilla and its associated olfactory sensory neurons**

447 We found that OSNs housed in pb1a sensilla from the mustard plant specialists *S. montana* and
448 *S. flava* respond to a broad range of ITC compounds (Figure 5 and Figure Supplement 5), and that this
449 sensilla type was numerically expanded in these two species (Figure Supplement 6-7). Concomitantly
450 with this, we discovered an increase in the number of *Or42a*-positive OSNs in *S. flava* compared to *S.*
451 *pallida* (Figure 6). Similar increases in OSNs which detect odors that bear species-specific biological
452 significance have been reported in several *Drosophila* species. For instance, the noni fruit specialist *D.*
453 *sechellia* and the seasonal specialist of "screw pine" (*Pandanus* spp.) fruits *D. erecta* both show an
454 increase in the number of *Or22a*-positive OSNs (Dekker et al. 2006; Linz et al. 2013; Auer et al. 2020).
455 In *D. sechellia*, these OSNs enhance odor tracking by reducing adaptation in second-order projection
456 neurons (Takagi et al. 2024). We hypothesize that the increase in the number of *Or42a*-positive OSNs in
457 *S. flava* may similarly contribute to enhance odor sensitivity and tracking during host plant finding,
458 although this remains to be investigated.

459

460 **3-4. Insight into the binding pocket of *S. flava* olfactory receptor Or42a paralogs**

461 Our results demonstrate that the Or42a paralogs from microbe-feeding species show strong
462 responses to both AITC and γ-hexalactone (Figure 7), while the paralogs from the herbivorous *S. flava*
463 show a notable shift in olfactory sensitivity, which aligns with the fact that this species has undergone a
464 full transition to herbivory. For example, *S. flava* Or42a3 showed a moderate response to γ-hexalactone
465 (although about an order of magnitude lower than that of the Or42a from the microbe-feeding *S.*
466 *pallida*), and *S. flava* Or42a4 was even less sensitive (Figure 7). Furthermore, *S. flava* Or42a4 had a
467 relatively higher sensitivity to butyl ITC compared to Or42a3 (Figure 7). To explore the mechanisms
468 underlying this shift from fruit-detector to ITC-detector, we employed computational and functional
469 approaches to identify the amino acid substitutions responsible for the differencial odor sensitivity of *S.*
470 *flava* Or42a3 and Or42a4.

471 Our AlphaFold2-led screening, combined with site-directed mutagenesis and
472 electrophysiological studies, identified two key substitutions in the transmembrane region of Or42a4,
473 A181D and S307P, that are critical for the odor sensitivity switch (Figure 8). Proline is a secondary
474 structure breaker (Chou and Fasman 1978; Levitt 1978), and the substitution of serine by proline

475 (S307P) likely influenced the conformation change of the binding pocket, altering the protein structure,
476 polarity, and hydrophobicity. Similarly, the substitution of alanine by aspartic acid (A181D) can alter
477 protein polarity and hydrophobicity. Thus, these two amino acid changes likely account for the notable
478 change in ligand sensitivity. However, this change in ligand sensitivity was observed only in flies
479 heterozygous for A181D and S307P (Or67d^{Gal4}; UAS-A181D S307P/+), but not in homozygous flies
480 (compare Figure 8C-D with Figure Supplement 12). Given that homozygous flies express A181D and
481 S307P more strongly than the heterozygous flies, it is possible that the OSNs' response to both odorants
482 reached saturation in the former, obscuring differences in spike ratios. Alternatively, excessive
483 expression of A181D and S307P may have altered the 3D structure of the heteromeric protein, possibly
484 through dominant-negative effects between the copies, reverting it closer to the original *S. flava* Or42a3
485 conformation and restoring the original binding pocket. Nonetheless, the partial rescue we observed in
486 heterozygous flies indicates that A181D and S307P are critical for altering the binding pocket structure,
487 enabling the Or to better accommodate butyl ITC instead of γ-hexalactone. Although the remaining
488 amino acid substitutions in Or42a4 might alter e.g. signal transduction and/or receptor stability, it is
489 remarkable that only two substitutions out of 32 amino acid differences between paralogs were sufficient
490 to shift ligand sensitivity.

491

492 **4. CONCLUSIONS**

493 Taken together, our findings reveal that non-herbivorous, microbe-feeding insects like *D.*
494 *melanogaster* have evolved promiscuous olfactory sensory mechanisms that allow them to detect and
495 avoid specialized plant-derived volatile electrophilic toxins, such as isothiocyanates. In contrast,
496 Brassicales plant specialists like *S. flava* not only have physiological adaptations to detoxify these toxic
497 compounds but have undergone significant evolutionary sensory adaptations for aiding host plant
498 location, including turning shifts and expansions of specialized isothiocyanate olfactory receptors.
499 Furthermore, our use of AlphaFold2, followed by site-directed mutagenesis and electrophysiology,
500 identified critical amino acid changes for the evolution of these specialized odorant receptors that we
501 confirmed experimentally. Thus, ancestral Ors that mediate toxin aversion in generalist species can be
502 co-opted and diversified in derived specialists through gene duplications and tuning shifts facilitated by
503 relatively few amino acids substitutions.

504

505

506 **5. MATERIAL AND METHODS:**

507 **Fly Husbandry**

508 *D. melanogaster* was reared on cornmeal medium. Microbe-feeding *S. pallida* (*S. pallida*
509 subgenus *Parascaptomyza*) and *S. hsui* (*S. hsui*subgenus *Hemiscaptomyza*) were reared in cornmeal
510 molasses media covered with a mixture of Carolina biological supply instant *Drosophila* media
511 (Burlington, NC) mixed with blended spinach leaves, and then covered with a layer of defrosted frozen
512 spinach leaves. The obligate leaf-miners *S. flava* and *S. montana* (subgenus *Scaptomyza*) were cultivated
513 on potted fresh laboratory-grown *Arabidopsis thaliana* Col-0. Isofemale lines of microbe feeding *S. hsui*
514 and *S. pallida*, as well as the herbivorous *S. montana,* were collected along Strawberry Creek on the UC-
515 Berkeley Campus in Berkeley, California, USA (Kim et al. 2021), and a line of *S. flava* was collected
516 from a meadow near Dover, New Hampshire, USA. All species were kept at 23±2 °C and 60% relative
517 humidity in a 10:14 hours light-dark cycle under fluorescent lights. The following lines (stock #) were
518 obtained from the Bloomington *Drosophila* Stock Center: *Or42a-/-* (60821), *Or42a-Gal4* (9970), w^{1118}
519 (3605), $TrpA1^{1}$ (26504), *Or7a-/-* (91811), and a genetic background control for the three *Or* null mutant
520 lines (68384). The *Or35a-/-* line (10564) was obtained from the Korea Stock Center. The $Or67d^{Gal4}$ line
521 was a gift from the laboratory of Barry J. Dickson.

522

523 **Single sensillum recordings (SSRs)**

524 One to five days old fed female flies were prepared for SSR as described in Matsunaga et al.
525 (2021). Briefly, a silicon tube delivering a constant flow of charcoal-filtered air (16 ml/min, measured
526 using a flowmeter, Gilmont Instruments, USA) was placed near the fly's head capsule, and the tip of the
527 stimulation pipette (50 ml) was inserted into the constant air stream. The stimulation pipette contained a
528 0.5 cm x 5 cm piece of filter paper loaded with 20 µl of an odorant solution or the solvent control. A
529 pulse of clean air (duration = 1 sec) was delivered to the stimulus pipette using a membrane pump
530 operated by a Stimulus Controller CS 55 (Syntech, Buchenbach, Germany). Sensilla identification was
531 conducted using the following diagnostic odorants (as described in Dweck et al. 2016; Gonzalez et al.
532 2016), all >95% pure (Sigma-Aldrich, St. Louis, MO, USA): ethyl acetate (CAS# 141-78-6) for
533 identifying *D. melanogaster* pb1a; AITC (CAS # 57-06-7) for identifying *Scaptomyza* pb1a-like OSNs;

534 4-ethylguaiacol (CAS# 2785-89-9) for identifying *D. melanogaster* and *Scaptomyza* pb1b and pb1-like
535 OSNs; fenchone (CAS# 1195-79-5) for identifying *D. melanogaster* and *Scaptomyza* pb2a and pb2a-like
536 OSNs; guaiacol (CAS# 90-05-1) for identifying *D. melanogaster* and *Scaptomyza* pb2b and pb2b-like
537 OSNs; phenethyl acetate (CAS# 103-45-7) for identifying *D. melanogaster* pb3b, *S. flava* pb3b-like, and
538 *S. montana* pb3b-like OSNs; and 2-heptanone for identifying *S. hsui* and *S. pallida* pb3a-like OSNs. All
539 odorants were diluted in mineral oil (CAS# 8042-47-5) except γ-hexalactone (CAS # 695-06-7), which
540 was diluted in dimethyl sulfoxide (CAS# 67-68-5) because it did not dissolve completely in mineral oil
541 and sometimes produced response artifacts. Odorants were diluted to 1:100 vol/vol for stimulation
542 unless otherwise noted. Supplementary file 1 lists all the chemicals used in this study.

543 The "net number of spikes/second" was obtained by counting the number of spikes originating
544 from the OSN of interest within a 0.5-second timeframe which started 0.2 seconds after the onset of
545 stimulation. This count was then adjusted by subtracting the background spiking activity (# of spikes
546 within a 0.5 second interval preceding the onset of the stimulation) and then doubled to represent the
547 number of spikes/second. In all figures, unless otherwise stated, we represent the "control-subtracted net
548 # of spikes/sec" to odorant stimulation, calculated by subtracting the average net # of spikes/sec in
549 response to the solvent control (mineral oil or dimethyl sulfoxide) from the net # of spikes/sec evoked
550 by each odorant stimulation. Control-subtracted spike data are compiled in Supplementary file 2. The
551 butyl ITC to γ-hexalactone spike ratio (Figure 8D and Figure Supplement 12) was calculated as: net # of
552 spikes/sec evoked by butyl ITC / (net # of spikes/sec evoked by butyl ITC + net # of spikes/sec evoked
553 by γ-hexalactone). We used this denominator for the ratio because the control-subtracted net # of spikes
554 upon γ-hexalactone stimulation occasionally produced negative values (likely a response to the solvent
555 control).

556 Half maximal effective concentrations (EC_{50}) were calculated using *Quest Graph™ EC50*
557 *Calculator* (AAT Bioquest, Inc., 4 Mar. 2025, https://www.aatbio.com/tools/ec50-calculator). We
558 primarily used the two-parameter feature with normalization, where responses were normalized to the
559 largest response within the same chemical-species pair, with the minimum set to 0. This approach was
560 chosen because the lowest tested concentration (10^{-5}) still elicited non-zero spike activity (>10) in some
561 chemical-species pairs. The four-parameter method without normalization, in which the maximum and
562 minimum responses were free parameters, was used in cases where the two-parameter method failed to
563 fit a logistic regression (summarized in Supplementary file 2) or when analyzing *sec*-butyl ITC data. For

564 this odorant, the four-parameter method was necessary because the highest tested concentration (10^{-2})
565 did not reach saturation (<100 spikes). When both the two-parameter and four-parameter methods failed
566 due to lack of convergence at the lowest concentration (10^{-5}), resulting in a calculated value of 0, we
567 instead used the minimum value observed within that chemical-species group.

568 The *Or67d*^{GAL4} line was used to generate flies expressing *Or42a* homologs in the at1 "empty
569 neuron" system (Kurtovic et al. 2007). We selected at1 (instead of the more commonly used antennal
570 basiconic ab3 "empty neuron system", Dobritsa et al. 2003) because some insects use host-derived
571 chemicals as pheromones (Reddy and Guerrero 2004), and in *D. melanogaster* pheromones sometimes
572 activate OSNs housed in trichoid sensilla only (Xu et al., 2005; Benton et al., 2007).

573 The spike amplitude differences between the two types of OSNs housed in pb3a-like and pb3b-
574 like sensilla were less distinct in *Scaptomyza*, and therefore we could not completely rule out the
575 possibility that we occasionally erroneously assigned spiking to each of these two OSNs types.

576

577 **Immobility assay**

578 To investigate the effect of AITC volatiles in wild-type *D. melanogaster* (Canton-S strain), we
579 used a 9 cm diameter plastic petri dish (Nunc, Denmark) with a piece of fabric mesh placed horizontally
580 between the base and the lid, creating two chambers (Figure Supplement 1A). The upper chamber
581 housed 8-10 male flies 3-5 days old, and the lower chamber contained four 5 µl drops of the odor
582 solution (or the solvent control) evenly dispersed. Because the mesh prevented the flies from reaching
583 the bottom chamber, insects were exposed to the volatile chemicals but could not directly contact (i.e.
584 taste) the odor solution, unless the molecules adhered to the walls of the chamber after volatilizing. After
585 each test started, we counted the number of mobile flies every 10 minutes up to one hour and calculated
586 the percentage of mobile flies at each time point. Flies exhibiting no movement for >30 seconds were
587 likely intoxicated. AITC and γ-hexalactone were respectively diluted in either mineral oil or dimethyl
588 sulfoxide at various concentrations. Mobility data analysis was performed using the log-rank (Mantel-
589 Cox) test (Mantel 1966). The complete immobility assay dataset is compiled in Supplementary file 3.
590

591 **Positional olfactory assay**

592 To study the olfactory orientation of insects towards odors, we conducted assays with non-
593 starved 3-4 days old mated females (Figure Supplement 1B). Flies (n=10-12/test) were anesthetized on
594 ice (5-7 minutes) and placed in a small piece of clear Tygon tube, capped in both sides with a conical
595 PCR plastic Eppendorf. After another about 4-5 minutes, the Tygon tube with the anesthetized flies was
596 uncapped and connected to the cut ends of two glass Pasteur pipettes and the assay started; flies usually
597 resumed activity after about 3-4 minutes. Each of the two opposite ends of the pipettes were respectively
598 connected to a 1.75-ml glass vial containing 10 µl of the odor solution (AITC 1: 500 vol/vol, or γ-
599 hexalactone 1:100 or 1:10 vol/vol) or 10 µl of the control solvent (mineral oil or dimethyl sulfoxide).
600 Tests with apple cider vinegar used 30 µl instead, and water was used as a control. The distal ends of the
601 pipettes were separated from the glass vials with a small piece of fabric mesh, which allowed the
602 odorant to diffuse into the pipettes while also preventing insects from contacting the odor source (Figure
603 Supplement 1B). The odor and control sides were switched between assays. Assays were conducted on a
604 white surface under white light at 21-24 °C, about 2-6 hours after lights on. Once each assay started, the
605 number of flies in the pipette closest to the vial with the odor (referred to as "odor side" or "odorous
606 tube" for simplicity), in the pipette closest to the vial with the solvent control ("control" side/tube), and
607 in the Tygon tube that connected both pipettes (release site) were counted every 5 minutes until minute
608 35, and then again at 65 minutes in the case of tests with AITC. For each assay, we calculated the % of
609 insects that made a choice for one or the other tube as: [(#of insects in the odor side + # of insects in the
610 control side) / total number of insects released] x 100. The percentage of insects that choose the odorous
611 tube was calculated based on the total number of insects that made a choice as: [# of insects in the odor
612 side / (# of insects in the odor side + # of insects in the control side)] x 100. Assays in which less than
613 40% of insects made a choice for either side at all time points were discarded (<5% of assays). For each
614 fly genotype and odorant, the % of insects that choose the odor side at each time point was compared
615 against the median value expected under the null hypothesis that insects distributed at random between
616 the two tubes (50% of insects in each tube) using one-sample signed rank tests. Thus, we assessed
617 whether the insects significantly avoided the odorous tube (if median<50%), preferred it (if
618 median>50%), or showed a random preference (median ca. 50%). In some cases, at each time point and
619 for each odor (and concentration when applicable), the responses of the null mutants (*Or42a-/-*, *Or7a-/-*
620 and *Or35a-/-*) and their genetic background control (line 6834 listed above) tested in parallel (i.e. in the
621 same days) were compared via Mann-Whitney U tests. In all cases results were considered significant if

622 $p<0.05$. In most cases we used two-tailed tests (e.g. for testing $median_1 \neq median_2$), but in a few cases
623 we used one-tailed tests (e.g. for specifically testing whether $median_1 > median_2$ or whether
624 $median_1<median_2$, Figure Supplement 2F-I). The positional olfactory assay data is included in
625 Supplementary file 4. In this and all behavioral assays, we used the line # 6834 instead of the more
626 standard *w1118*, because the latest have visual defects that interfere with normal behavior (Ferreiro et al.
627 2017).
628
629 **Consumption assay**
630 This behavioral assay (described in Reisenman and Scott 2019) measures if the presence of an
631 odorant affected consumption of an appetitive solution. Groups of 2-4 days old mated female flies
632 (n=11-15) were wet-starved for 24 hours and then transferred to a vial containing a piece of filter paper
633 (2.7 cm diameter, Whatman, cat. No 1001 125) impregnated with 160 µl of 50 mM D-glucose (Sigma-
634 Aldrich, USA) dyed blue with Erioglaucine (0.25 mg/ml, Sigma-Aldrich, St. Louis, MO, USA; Figure
635 Supplement 1C). Flies were allowed to feed for 15 minutes (10 minutes in tests with γ-hexalactone),
636 frozen (>60 minutes), and the amount of blue dye in the flies' abdomen was scored blind to treatment
637 (see below). The odor source consisted of a strip of filter paper (0.25 cm wide x 1.5 cm long)
638 impregnated with either 10 µl of an odorant solution (test) or 10 µl of the solvent (control), which was
639 placed inside a container (1.3 cm long x 0.75 cm diameter) with a meshed bottom affixed to the vial's
640 flug (Figure Supplement 1C). This allowed diffusion of odors into the fly vial but prevented flies from
641 contacting the odor source. Control tests, with vials containing food solution but only the solvent control
642 inside the meshed container, were conducted in parallel with experimental tests to control for fly cohort
643 and day-to-day variability.
644 Food consumption was estimated by scoring individual flies in each vial blind to treatment using
645 the following five-point scale (Reisenman and Scott 2019): 0 (no dye = no food), 0.25 ("trace" of blue
646 dye), 0.5 (up to ¼ of the abdomen dyed blue), 1 (more than ¼ but less than ½ of the abdomen dyed
647 blue), and 2 (more than ½ of the abdomen dyed blue). For each vial, a single feeding score value was
648 calculated as: $[(0 \times n_0 + 0.25 \times n_{0.25} + 0.5 \times n_{0.5} + 1 \times n_1 + 2 \times n_2) / N]$, where $n_{(0-2)}$ denotes the number of
649 flies in each score category, and N the total number of flies/vial. Feeding scores from each test vial (flies
650 offered food in presence of an odor) were normalized to the averaged feeding score of control vials (flies
651 of the same genotype offered food in absence of odor) assayed on the same day. Normalized feeding
652 scores for each genotype and odor were compared against the null hypothesis (median feeding score = 1)

using one sample signed rank tests. That is, medians not different from 1 indicate that the odorant did not reduce neither enhanced consumption, while medians significantly less than 1 or more than 1 respectively indicate feeding aversion and enhancement. Normalized data from control and mutant flies were compared using Mann-Whitney U tests. In all cases results were considered statistically significant if $p<0.05$. The consumption assay data is compiled in Supplementary file 5.

RNA-sequencing of maxillary palps

Newly emerged adults of *S. flava* and *S. pallida* were collected from our colony and kept in humidified vials with 10% honey water until dissection, to minimize potential differences in nutrition resulting from differences in the two species' larval diet. Three- ten days old flies were anesthetized with CO_2, and their maxillary palps were hand-dissected using forceps. Approximately 100-120 flies were pooled for a single sample. The dissected tissues were directly collected in LB+TGA lysis buffer from Reliaprep RNA Tissue Miniprep System (Promega, USA), and homogenized using a Biomasher Standard homogenizer (Takara Bio Inc., USA) in a dry ice ethanol bath. The sample lysates were stored at -80°C until RNA extraction. Total RNAs were extracted from the lysates using ReliaPrep RNA Tissue Miniprep System (Promega, USA) according to the manufacturer's protocol, and quantified using a Qubit RNA High Sensitivity kit (Thermo Fisher Scientific, USA). Library preparation was performed at the Functional Genomics Laboratory at UC Berkeley. Due to the low yields of our maxillary palp-derived total RNAs, cDNA libraries were first produced by Takara SMART-Seq mRNA Ultra-low input RNA kit (Takara Bio Inc., USA) with 8 cycles of PCR for the amplification, and then processed by KAPA HyperPrep kit for DNA (Roche Sequencing, USA) with 9 cycles of PCR for attaching in-house sequencing adapters and index primers. cDNA libraries were then sequenced on an Illumina NovaSeq 6000 150 PE S4 flowcell, targeting 25M read pairs per library by the UC Berkeley Vincent J. Coates Genomics Sequencing Laboratory. For read mapping, we used previously reported reference genome assemblies and gene annotations from *S. flava* (Peláez et al. 2023) and *S. pallida* (Kim et al. 2021) for subsequent bioinformatic analyses. Raw RNA-seq reads were filtered using Fastp v0.21.0 (Chen et al. 2018) and mapped to the respective reference genomes using STAR v2.7.1a (Dobin et al. 2013) to generate multiple alignment (BAM) files, which were then converted to read count data using HTseq v0.9.1 (Anders et al. 2015). Count data for the *Or* gene family were converted to RPM (reads per million; Supplementary file 6).

684 **Hybridization chain reaction RNA Fluorescent in situ hybridization (FISH)**

685 One- four days old female *S. flava* and *S. pallida* were collected and anesthetized with CO_2.
686 Whole mouthparts were removed and immediately placed in 2 mL of fixative (4% vol/vol
687 paraformaldehyde in 1x phosphate buffer saline with 3% vol/vol Triton X-100 added, PBST) in LoBind
688 Eppendorf tubes, and fixed for 22 hours at 4°C on a nutator. For HCR RNA fluorescent in situ
689 hybridization, we followed the manufacturer's instruction (Molecular Instruments, Inc., Los Angeles,
690 CA).

691 Samples were stained with 300 nM DAPI in 0.1% PBST for 15 minutes and then washed 3 times
692 with 0.1% PBST for 5 minutes. Tissues were transferred to a microscope slide and mounted in a drop of
693 ProLong diamond antifade mounting (Life Technologies Corp., Eugene, OR) and stored at 4°C until
694 examination. Confocal imaging of fixed samples was performed using a Zeiss LSM 880 microscope in
695 the AiryScan mode. Raw images were processed using Zeiss ZEN Black software. Orco-positive cells
696 (visualized with the 488 nm laser) and Or42a-positive cells (visualized with the 633 nm laser) were
697 manually counted using the "Cell Counter" plugin in Fiji (ImageJ) software. Supplementary file 7
698 contains cell counts from RNA Fluorescent in situ hybridization experiments.

699

700 ***Scaptomyza Or42a* gene cloning and generation of *UAS* lines**

701 RNA was isolated from 15-25 days old laboratory-reared adults of both sexes of *S. pallida* and *S.*
702 *flava* using the ReliaPrep Miniprep system (Promega, W.I., USA). Complementary DNA (cDNA) was
703 synthesized using the qScript cDNA Supermix (Quantabio, Beverly, MA, USA). The paralogs were
704 amplified via touchdown PCR, using primers that target the highly variable regions of the 5' and 3'
705 untranslated regions (UTRs). The single *Or42a2* gene of *S. pallida* was amplified using touchdown PCR
706 with primers targeting the coding region (Q5 DNA Polymerase, #M0491, NEB) (Supplementary file 8).
707 All PCR products underwent gel purification (11-300C, Zymo Research) and were subsequently cloned
708 using the Gibson Assembly (E2611S, NEB) following the manufacturer's instructions into the UAST-
709 attB vector (DGRC Stock 1419; RRID:DGRC1419, Bischof et al. 2007). The ligation products were
710 transformed into DH5α competent cells (T3007, Zymo Research). After confirming the sequences using
711 Sanger sequencing, the 5' and 3' UTRs of the plasmids containing the *S. flava Or42a* paralogs were
712 removed. This was achieved by first amplifying the coding region using PCR, followed by gel
713 purification and ligation back into UAST-attB vector via Gibson Assembly. The resultant plasmids were

714 verified using Sanger sequencing. Finally, these plasmids were microinjected into the attP40 site (P{nos-
715 phiC31\int.NLS}X, P{CaryP}attP40, line # 25709, Rainbowgene) to create transgenic lines for *S.*
716 *pallida Or42a*, *S. flava Or42a2*, *S. flava Or42a3* and *S. flava Or42a4*. All lines were confirmed by
717 Sanger sequencing prior to experiments.

718

719 **Screening of candidate amino acids using AlphaFold2 3D structural prediction**

720 CDS of *S. flava Or42a3* and *S. flava Or42a4* were confirmed by palp RNAseq data using
721 IGV_2.16.0. CDSs of *S. flava Or42a3* and *S. flava Or42a4* were then used as inputs into ColabFold
722 (Jumper et al. 2021; Mirdita et al. 2022). Then the output models ranked first (rank1) were selected,
723 visualized, and 3D-aligned by using PyMol2.5.3. We focused on the regions where predicted local
724 distance difference test scores exceed 70, as structures with lower values are often unreliable (Mariani et
725 al. 2013). We focused on the S5-S6 transmembrane helices because previous studies suggested that the
726 binding pockets of odorant receptors are located in the transmembrane region (Butterwick et al. 2018;
727 Del Mármol et al. 2021; Zhao et al. 2024), and our amino acid alignment of *S. flava* Or42a3 and *S. flava*
728 Or42a4 provided the highest root mean square deviation scores in this region. In silico substitutions of
729 amino acids were performed individually on *S. flava* Or42a3, and the resulting sequences were then re-
730 input into ColabFold, the model with rank1 was selected, and the structures were 3D-aligned with that of
731 *S. flava* Or42a4. This process of in silico mutation and alignment was repeated until the root mean
732 square deviation scores for the S5-S6 region were reduced to a value comparable to the other region
733 (~0.1 Å). All pdb files used in this study are included in Supplementary file 9.

734

735 **Site-directed mutagenesis**

736 Conventional PCR was conducted using plasmids of *S. flava Or42a3* as backbone (Q5 DNA
737 polymerase, #M0491, NEB; Supplemental File 1). Primers were designed to introduce the point
738 mutations (Supplementary file 1). The PCR product underwent gel purification (11-300C, Zymo
739 Research) and the methylated plasmids were digested with DpnI for 1 hour at 37°C (QuickChange,
740 Agilient Technology, USA). Ligation was performed by incubation at 16°C for 30 minutes (DNA
741 ligation kit Mighty mix, Takara, Japan) and the products were transformed into DH5α competent cells
742 (Takara, Japan). After confirming the sequence using Sanger sequencing, the plasmid was microinjected

743 into the attP40 site (P{nos-phiC31\int.NLS}X, P{CaryP}attP40, line # 25709, Rainbowgene) to create
744 the mutant A181D S307P fly line. The mutations were confirmed by sequencing prior to experiments.

745

746 **ACKNOWLEDGEMENTS:**

747 We are grateful to two anonymous reviewers and to the editor for their constructive comments and
748 suggestions that improved this manuscript. T.M. thanks Hany Dweck for valuable insights about
749 conducting SSR of maxillary palp sensilla, to Dr. Akinao Nose and Dr. Hiroshi Kohsaka for their advice
750 and encouragement, and to the members of the Nose' laboratory and an anonymous researcher at the
751 University of Tokyo for discussions. We thank members of the Whiteman and Scott Laboratories for
752 discussions and comments on the manuscript. The Bloomington Drosophila Stock Center, the Korean
753 Stock Center, and the Drosophila Genomics Resource Center (NIH Grant 2P40OD010949) kindly
754 provided fly lines. We are grateful to T. Michael Keesey for the use of *A. thaliana* silhouette in
755 PhyloPic. This work was supported by the Grant-in-Aid for Scientific Research Activity Start-up (T.M.),
756 the Uehara Memorial Foundation (award number 201931028 to T.M.), the National Institute of Health
757 (NIH) Grant (award number R35GM139653 to Gary Karpen), and the National Institute of General
758 Medical Sciences of the NIH (award number R35GM119816 to N.K.W.).

759

760 **AUTHORS' CONTRIBUTION:**

761 All authors contributed to the experimental design, analysis, and interpretation of results. T.M. initiated
762 the project and performed all experiments, except for the behavioral experiments (Fig. 4, Fig.
763 Supplement 2A-J, and others indicated in the text and/or Figure captions), which were conducted by
764 C.E.R. RNA fluorescent in situ hybridization experiments (Fig. 6C-E) were performed by B.G.H. and
765 S.R.; RNA-seq analysis (Fig. 6B) was performed by H.C.S. D.T. cloned *UAS-Or42a*s. J.W. contributed
766 to the behavioral experiment presented in Fig. 4B. S.R.R. provided advice on SSR to T.M. T.M. wrote
767 the manuscript in its original and revised versions with a substantial contribution from C.E.R.; C.E.R
768 also wrote and revised the sections corresponding to the experiments she conducted. All authors,
769 especially N.K.W. and C.E.R., provided feedback on the overall manuscript. N.K.W. supervised T.M.
770 during the initial stages of the project.

771

772

773 **FIGURE CAPTIONS:**

774

775 **Figure 1: Questions addressed in this study.**

776

777 **Figure 2: *Drosophila melanogaster* is immobilized rapidly upon exposure to volatile allyl**
778 **isothiocyanate.**
779 The toxic effect of various concentrations (vol/vol) of volatile AITC to *D. melanogaster* was assessed by
780 measuring the % of mobile flies; flies were not allowed to contact the AITC source (Figure Supplement
781 1A). Increasing the concentration of AITC decreases the % of mobile flies, likely due to intoxication.
782 n=10 for each condition (solvent and concentration). **** $p<0.0001$, log-rank Mantel-Cox tests against
783 the control.

784

785 **Figure 3: *Drosophila melanogaster* Or42a mediates detection of volatile allyl isothiocyanate.**
786 **(A)** Schematic and representative trace of a single sensillum recording (SSR) from pb1 OSNs upon
787 stimulation with AITC 1:100 vol/vol. The horizontal bar indicates the onset of the stimulus and its
788 duration (1 sec). **(B)** SSR from all *D. melanogaster* antennae and palp basiconic sensilla upon AITC
789 stimulation (1:100 vol/vol; n= 6-10 recordings/sensilla type from 6 animals). Represented here and in all
790 figures are the control-subtracted net number of spikes/sec, unless otherwise noted. The horizontal
791 dotted line at zero indicates no response to odor stimulation. Here and thereafter, horizontal bars
792 represent the median, the edges of the boxes correspond to 25th and 75th quartiles, the whiskers denote
793 10th and 90th quartiles, and symbols indicate outliers. Pb1a sensilla, which house Or42a (Ray et al.
794 2007), respond strongly to AITC. **(C)** Responses from pb1 sensilla of wildtype Canton-S, the genetic
795 background control w^{1118}, *Or42a-/-*, and $TrpA1^{1}$ *D. melanogaster* flies to 1:100 vol/vol AITC
796 stimulation (n=6-10 sensilla/genotype from 3-4 animals/genotype). The responses of both mutant flies
797 were compared against each other and against those of *w1118*. Kruskal-Wallis ANOVA followed by
798 Dunn's multiple comparisons, *$p<0.05$, **$p<0.01$.

799

800 **Figure 4: *Drosophila melanogaster* Or42a mediates behavioral aversion to allyl isothiocyanate.**
801 **(A)** Positional olfactory assay. Flies could smell, but not contact, the AITC solution (Figure Supplement
802 1B). The number of flies in the odorless and the odorous glass tubes was counted every five 5 minutes
803 until minute 35, and then again at 65 minutes. The dotted line at 50% indicates random distribution
804 between the two tubes. Genetic background control flies (line # 68384, blue boxes, n=15) avoided the
805 tube closest to the odor source at various time points (***$p<0.005$, ****$p<0.001$; one-sample signed
806 rank tests against median=50%). *Or42a-/-* mutants (orange boxes, n =15) distributed randomly between
807 the two tubes at all timepoints ($p>0.05$) except at 65 minutes (*$p<0.01$). **(B)** Food consumption assay in
808 presence or absence of AITC volatiles (1:500 vol/vol). Flies could smell but not contact the AITC
809 solution (Figure Supplement 1C). Both genetic background control flies (n=16) and *Or42a -/-* mutants
810 (n=14) fed less in the presence of AITC volatiles (medians<50%, one-sample signed rank tests on
811 normalized data; respectively $p<0.05$ and $p<0.001$), but the feeding score of genetic control flies was
812 lower than that of mutant flies (Mann-Whitney U test, ***$p<0.001$). The dotted line at 50% indicates no
813 feeding aversion or enhancement.

814

815 **Figure 5: Maxillary palp pb1-like sensilla of the mustard plant specialist *Scaptomyza* species have**
816 **an expanded ITC-sensitivity range.**
817 Single sensillum recordings from maxillary palp pb1 OSNs of *D. melanogaster, S. hsui, S. pallida, S.*
818 *flava,* and *S. montana*. Stimuli (1:100 vol/vol) included diagnostic chemicals used to identify Ors in *D.*
819 *melanogaster* (see Methods), fruit volatiles, green leaf volatiles, and Brassicales plant-derived
820 isothiocyanates (ITCs) (n=6-9 from 3-4 animals/species). Pb1 and pb1-like sensilla housed two OSNs,
821 labeled "a" (darker color) and "b" (lighter color). See methods for sensilla classification and the Figure
822 supplement 3-4 for functional characterization of pb2 and pb3. While pb1a OSNs from all species
823 responded to AITC, pb1a-like OSNs from the mustard plant specialists *S. flava* and *S. montana*
824 additionally responded to other ITC compounds. Mustard specialization occurred at the clade leading to
825 the common ancestor of these two species, denoted by the leaf cartoon. Because sensilla with extremely
826 small spike amplitudes were excluded from analysis, additional unidentified palp basiconic sensilla may
827 exist in *Scaptomyza*. AITC: allyl ITC, IBITC: isobutyl ITC, BITC: butyl ITC, SBITC: *sec*-butyl ITC,
828 PITC: phenethyl ITC. The structure of ITCs is shown in Figure Supplement 5.
829

830 **Figure 6: High expression of *Or42a* paralogs and over-representation of *Or42a*-positive OSNs in**
831 **the maxillary palp of *S. flava*.**
832 **(A)** Schematic of *Or42a* syntenic regions in the genomes of the microbe-feeding *S. pallida* and the
833 mustard plant specialist *S. flava*, with a gene triplication in the *S. flava* genome at the syntenic region of
834 *S. pallida Or42a2* (*S. flava Or42a2*, *S. flava Or42a3*, and *S. flava Or42a4*). **(B)** Maxillary palp RNA seq
835 of *S. pallida* and *S. flava Or*s (n=3 replicates/sex and species). *Or*s with median values of the log2 (RPM
836 +1) < 1 (n=3) were excluded. *S. pallida* expresses only one copy of Or42a, while the specialist *S. flava*
837 expresses three copies. **(C-C")** Representative images of hybridization chain reaction RNA fluorescent
838 in situ hybridization from the maxillary palps of *S. pallida* and *S. flava* showing *Or42a*-positive OSNs
839 (**C**, green), *Orco*-positive OSNs (**C'**, magenta**),** and the merged signals (**C'',** white indicates co-
840 localization of *Or42a*-positive OSNs and *Orco*-positive OSNs). Or42a is expressed in OSNs. Scale bar:
841 20µm. **(D-E)** Number of *Or42a*-positive OSNs and *Orco*-positive OSNs in the maxillary palps of *S.*
842 *pallida* (blue boxes) and *S. flava* (orange boxes) **(D),** and ratio between them **(E)**. Mann-Whitney U
843 tests, ** p<0.01; n=5 animals/species. *S. flava* has more Or42a-positive OSNs and more Orco-positive
844 OSNs than *S. pallida*.

845

846 **Figure 7: Functional characterization of the olfactory receptor Or42a from *D. melanogaster*, *S.***
847 ***pallida*, and *S. flava.***
848 **(A)** Representative SSR traces from *D. melanogaster* at1 sensilla OSNs expressing species-specific
849 *Or42a* under the control of *Or67d* ^{Gal4} (fly genotype: *UAS-Or42a; Or67d* ^{Gal4}) in response to stimulation
850 with butyl isothiocyanate (BITC) and the fruit odor γ-hexalactone. The horizontal bars above records
851 indicate the onset and duration (1 sec) of the stimulation. **(B)** Responses of at1 OSNs (n=6-8 sensilla
852 from 3-4 animals/genotype) expressing species-specific *Or42a* upon stimulation with *trans*-2-hexenal (a
853 general leaf odor released upon leaf mechanical damage such as crushing), various ITCs produced by
854 mustard plants (AITC, IBITC, BITC, SBITC, abbreviations as in Figure 5), and γ-hexalactone.
855 Orthologs from all species respond to AITC, while *S. flava* Or42a3 and *S. flava* Or42a4 additionally
856 respond to various ITCs. In contrast, only paralogs from microbe feeding species show strong responses
857 to γ-hexalactone.
858

859 **Figure 8: Two amino acids are critical for changing the sensitivity of *S. flava* paralogs from fruit**
860 **volatiles to isothiocyanates.**

861 **(A-A')** The 3D alignment of *S. flava* Or42a3 and *S. flava* Or42a4 predicted by AlphaFold2 **(A)**, and 3D
862 alignment of *S. flava* Or42a4 and a chimeric Or42a with two amino acid substitutions (A181D and
863 S301P) in the background of *S. flava* Or42a3 **(A')**. The root mean square deviation is visualized with a
864 color gradient from blue (low) to red (high) in both the side (left) and the top view (right). The upper
865 and lower sections of the side view respectively represent the extracellular and the intracellular regions
866 separated by the cell membrane (gray rectangles). **(B-D)** Representative single sensillum recording from
867 *D. melanogaster* at1 sensilla expressing heterologous *S. flava* Or42a3, Or42a4, and the chimera
868 (genotype: *UAS-Or42a/CyO; Or67d* ^{Gal4}) upon stimulation with butyl isothiocyanate (BITC) and γ-
869 hexalactone (**B**), at1 population responses to BITC (white bars) and to γ-hexalactone (gray bars) (**C**,
870 n=6-10 sensilla from 3-4 animals/genotype; * $p<0.05$, Mann-Whitney U tests), and spike ratio [**D**,
871 (response to BITC) / (response to BITC + response to γ-hexalactone); ** $p<0.01$, *** $p<0.001$, Kruskal-
872 Wallis ANOVA followed by Dunn's multiple comparisons]. The odor tuning of the chimera, with just
873 two amino acid substitutions, recapitulates that of *S. flava* Or42a3.
874
875 **FIGURE SUPPLEMENT CAPTIONS:**

876 **Figure Supplement 1: Schematic representations of the behavioral assays. (A)** Mobility assay used
877 as a proxy for intoxication. Mated female flies (n=10) were placed in the upper chamber (lateral view)
878 and monitored every 10 minutes in presence of volatile chemicals (4 drops of a 5 µl solution in the lower
879 chamber, top view). The top and the bottom chambers were separated by a fabric mesh, preventing
880 direct contact between the flies and the chemical solutions. **(B)** Positional olfactory assay. Groups of 10-
881 12 non-starved cold-anesthetized mated females were placed in a small piece of clear Tygon tube, which
882 was then used to connect the narrow ends of two cut glass Pasteur pipettes (non-choice/release zone).
883 The distal end of each glass pipette was connected to a glass vial containing 10 µL of the odor solution
884 or the solvent control; a piece of fabric mesh prevented insects from entering the vials containing the
885 odor or control solutions. The number of flies in each of the two tubes, as well as in the middle release
886 section, were counted every five minutes until minute 35, and in tests with allyl ITC, again at 65
887 minutes. The % of insects that choose one or the other tube over the total number of insects released,
888 and the % of insects in the tube closest to the odor source over the total number of insects that choose
889 one or the other tube, was then calculated for each time point. **(C)** Feeding assay in presence of odors or
890 the solvent control. In each test a group of 24 hours wet-starved mated female flies (n=11-15) was
891 placed in a vial containing a piece of filter paper impregnated with 160 µl of 50 mM D-glucose dyed

892 blue. A small container with a mesh bottom was affixed to the inner side of the vial cap contained a
893 piece of filter paper loaded with 10 µl of an odorant solution or the solvent control, such as that flies
894 could smell but not contact the odor source. After 15 minutes, vials were frozen for at least 60 minutes,
895 the amount of blue dye in the abdomen of each fly in each vial was quantified blind to treatment, and a
896 feeding score was calculated for each vial as explained in materials and methods.

897

898 **Figure Supplement 2: Behavioral data related to Figure 4.** Positional olfactory assays. **(A-B)** Tests
899 with allyl isothiocyanate (AITC) 1:500 vol/vol vs mineral oil (as in Figure 4A) using Canton-S flies
900 (n=19); flies preferred the odorless tube from minute 25 onwards (one sample signed rank tests against
901 median=50%, *p<0.05 in all cases; **A**). Total choice of Canton-S flies calculated as: [(# of flies in the
902 odorless tube + # of flies in the odorous tube) / (# of flies released) *100)]; **B**. **(C)** Total choice of
903 genetic background control (line # 68384) and *Or42a-/-* mutants (n=15 for each genotype). Similar
904 percentages of control flies and *Or42a-/-* mutants choose one or the other tube at all time points,
905 indicating that all fly genotypes are similarly active in presence of AITC volatiles (Mann-Whitney U
906 tests, p>0.05 for all time points). **(D-E)** Tests using γ-hexalactone 1:10 vol/vol vs the solvent control
907 using genetic background control flies and *Or42a-/-* mutants. Control flies choose the odorous tube at 20
908 and 30 minutes (n=19, *p<0.05, one-sample signed rank tests), while mutants distributed randomly at all
909 time points (n=19, p>0.05 in all cases); **D**. Additionally, the total choice of control flies was larger than
910 that of mutant flies at all time points, suggesting that the presence of the odor increases exploration
911 activity in control flies (Mann-Whitney U tests, *p<0.05, ***p<0.005); **E**. Canton-S flies also showed
912 attraction to this odor (at 5, 10, and 15 minutes, n=12; one-sample signed rank tests, p<0.05 at all those
913 three times, data shown in Supplementary File 4). **(F-G)** Tests with *Or7a-/-* (n=15) and genetic
914 background control flies (n=18) using AITC 1:500 vol/vol vs mineral oil. Control flies avoided the
915 AITC tube at all time points, while mutants only avoided at 30 minutes and onwards (one-sample signed
916 rank tests, 1-tail, *p<0.05, ****p<0.001); **F**. The total choice of flies was not different between
917 genotypes (p>0.05 at all time points); **G**. **(H-I)** Tests with *Or35a-/-* (n=29) and genetic control flies
918 (n=27) using γ-hexalactone 1:10 vol/vol vs the solvent control. Control flies choose the odorous tube at
919 various time points (*p<0.05, ***p<0.001, one sample signed rank tests, 1 tail), while mutants always
920 distributed at random (p>0.05 in all cases); **H**. **I:** Total choice of control and Or35a-/- mutants;
921 differences between genotypes were not statistically different (Mann-Whitney U tests, p>0.05 at all time

922 points). In all cases (panels **C-I,** Figure 4A) mutants of the various genotypes used were assayed in
923 parallel with the genetic background control line and therefore, control data was obtained from different
924 subsets of flies. **(J)** Feeding assay, as in Figure 1E, but using γ-hexalactone (1:50 vol/vol). The dotted
925 line at 50% indicates neither feeding enhancement or repellence. Canton-S flies consumed more in
926 presence than in absence of γ-hexalactone (one-sample signed rank test on normalized data against
927 expected median=1, $p<0.001$, n=25), and *Or42a-/-* mutants instead consumed less in presence of the
928 odor; $p<0.001$, n=24). (**K)** Mobility assay, as in Figure 2, but using γ-hexalactone at various
929 concentrations from 1:500 to 1:2.5 vol/vol. n=10 for each condition (solvent and concentration). Flies
930 remained active in the presence of this volatile. **(L)** Single sensillum recordings from all *D.*
931 *melanogaster* antennae (ab) and palp basiconic (pb) sensilla upon stimulation with γ-hexalactone 1:100
932 vol/vol. Only pb1a was activated by γ-hexalactone (n= 3-6 OSNs). **(M)** Activation of Or42a, in
933 combination with distinct olfactory channels, is involved in mediating both olfactory repellence to AITC
934 (light blue arrow) and attraction to γ-hexalactone (orange arrow). Activation of Or42a in combination
935 with Or7a or O35a likely mediates repellence and attraction, respectively.
936
937
938 **Figure supplement 3: Functional characterization of *D. melanogaster* and *Scaptomyza* species**
939 **maxillary palp OSNs housed in the three palp basiconic sensilla types.**
940 Single sensillum recordings from maxillary palp OSNs (pb2, pb2-like, pb3, and pb3-like) of *D.*
941 *melanogaster, S. hsui, S. pallida, S. flava,* and *S. montana*. Stimuli (1:100 vol/vol) included diagnostic
942 chemicals used to identify Ors in *D. melanogaster* (see Methods), fruit volatiles, green leaf volatiles, and
943 Brassicales plant-derived isothiocyanates (ITCs) (n=6-9 from 3-4 animals/species). Pb and pb-like
944 sensilla housed two OSNs, labeled "a" (darker color) and "b" (lighter color). Their response profiles and
945 stereotyped locations within the palp support the classification of *Scaptomyza* sensilla into three types,
946 pb1-like, pb2-like, and pb3-like (see also Figure 5). Methyl salicylate (a *S. flava* volatile attractant in
947 natural settings, Orre et al. 2010) activated all *Scaptomyza* pb2b-like sensilla but not *D. melanogaster*
948 pb2b (first row). The response profiles of *Scaptomyza* pb3-like OSNs were different from those of *D.*
949 *melanogaster* pb3, likely because the homologs of *Or59c* and *Or85d*, which are respectively expressed
950 in *D. melanogaster* pb3a and p3b, are unidentified in the genomes of *Scaptomyza* (Goldman-Huertas et
951 al. 2015). The odorant response profiles of OSNs in pb3-like sensilla were more similar between the
952 more distantly related species *S. hsui* and *S. pallida,* than between the more closely related *S. pallida* and

953 *S. flava,* or *S. pallida* and *S. montana.* For example, *trans*-2-hexenal activated these OSNs in *S. hsui* and
954 *S. pallida* (but not in *S. flava* or *S. montana*), while phenethyl acetate activated *S. flava* and *S. montana*
955 OSNs (but not *S. hsui* or *S. pallida*). AITC: allyl ITC, IBITC: isobutyl ITC, BITC: butyl ITC, SBITC:
956 *sec*-butyl ITC, PITC: phenethyl ITC.
957
958
959 **Figure Supplement 4: Hierarchical cluster analysis of maxillary palp sensilla based on odorant**
960 **response profiles across species. (A)** Hierarchical clusters were constructed using odorant response
961 data from single sensillum recordings of basiconic palp sensilla from *D. melanogaster, S. hsui, S.*
962 *pallida, S. flava,* and *S. montana* using R studio v1.4.1717. A terminal node corresponds to a single
963 recording from the individual sensilla; n=6-8 sensilla from 3-4 animals. **(B)** Hierarchical clusters were
964 created for each sensilla type, including pb1-like, pb2-like, and pb3-like, using the odorant response
965 (control-subtracted net number of spikes) average from each species as inputs. **(C)** The species
966 phylogeny (left: Kim et al., 2021) and palp functional dendrogram (right) highlight the relevance of
967 niche differences in shaping odorant responses. The palp functional dendrogram was generated using
968 odorant response averages from each species.
969
970 **Figure Supplement 5. Responses of OSNs from *D. melanogaster* pb1a and *Scaptomyza* pb1a-like**
971 **sensilla to stimulation with various odorant concentrations. (A)** Responses of pb1a OSNs across
972 species upon stimulation with various concentrations (ranging from $1:10^{-2}$ to 10^{-5} vol/vol) of ethyl
973 butyrate, γ-hexalactone, *trans*-2-hexenal, allyl isothiocyanate (AITC), isobutyl isothiocyanate (IBITC),
974 butyl isothiocyanate (BITC) and *sec*-butyl isothiocyanate (SBITC; n=6-8 sensilla from 3-4
975 animals/species). The chemical structures of each compound are shown on the left. IBITC, BITC, and
976 SBITC were only tested in *S. flava* and *S. montana* pb1a, as BITC at 10^{-2} vol/vol failed to activate OSNs
977 in pb1a from the two microbe-feeding species (Figure 5). **(B-C)** Responses of *S. flava* and *S. montana*
978 pb1a OSNs upon stimulation with γ-hexalactone 10^{-4} vol/vol **(B)** and the green leaf volatile *trans*-2-
979 hexenal 10^{-4} vol/vol **(C)**; n=6-7 sensilla from 3 animals/species. Mann-Whitney U tests: *$p<0.05$,
980 **$p<0.01$. **(D)** Half maximal effective concentrations (EC_{50}) for each fly species and odorant (see
981 Methods for calculations of EC_{50}). Kruskal-Wallis tests followed by Dunn's multiple comparisons.
982 Different letters indicate significant differences between species (p-values for ethyl butyrate: *S. pallida*
983 vs *S. flava* $p<0.05$, *S. pallida* vs *S. montana* $p<0.01$; for γ-hexalactone: $p<0.001$; for *trans*-2-hexenal: *D.*

984 *melanogaster* vs *S. montana* p<0.05, *S. hsui* vs *S. flava* p <0.01, *D. melanogaster* vs *S. flava* p<0.0001;
985 for AITC: p<0.05). The EC_{50s} of *S. flava* and *S. montana* to BITC, IBITC and SBITC were not
986 statistically different (Mann-Whitney U tests, p>0.05). Overall, pb1a OSNs of microbe-feeding species
987 exhibited greater sensitivity to γ-hexalactone, whereas Brassicales specialists showed higher sensitivity
988 to *trans*-2-hexenal and AITC. *S. flava* and *S. montana* showed similar sensitivities to all four ITCs
989 tested.
990
991 **Figure Supplement 6: Or42a gene tree constructed by RAxML, and syntenic maps and dot plots**
992 **visualized by DiGAlign. (A)** Maximum-likelihood gene tree with 1000 bootstrap cycles using *S. hsui*
993 *Or42a1*, *S. pallida Or42a1*, *S. graminum Or42a1*, *S. montana Or42a1*, *S. flava Or42a1*, *S. hsui Or42a2*,
994 *S. pallida Or42a2*, *S. graminum Or42a2*, *S. flava Or42a2*, *S. montana Or42a*, *S. flava Or42a2*, *S. flava*
995 *Or42a3*, *S. flava Or42a4*, and *D. melanogaster Or42a* as an outgroup, generated by RAxML (v8.2.19)
996 (Stamatakis 2014) after alignment by MAFFT v7 (Katoh and Standley 2013). Bootstrap values are
997 shown on the branches when the values were lower than 80. The tree was displayed by FigTree v1.4.3
998 (Rambaut 2009). **(B)** Dot plots (left) and synteny maps (right) were generated for the *Or42a2-Or42a4*
999 genomic region across four species pairs: *S. flava-S. montana*, *S. montana-S. graminum*, *S. graminum-S.*
1000 *pallida*, and *S. pallida-S. hsui*. A 60,199-nt region was analyzed in *S. flava*, and 30,000-nt regions were
1001 analyzed in the other four species. Genomes of *S. montana, S. graminum,* and *S. pallida* were reversed-
1002 aligned for visualization. Each genomic region is color-coded according to BLASTn percent identity
1003 (top left). Cyan rectangles mark the span from the start to the end of *Or42a* homologs. *S. flava* has three
1004 copies of *Or42a2* species-specific, separated by intronic intervals that are mostly not conserved in the
1005 other species. In contrast, the remaining *Scaptomyza* species showed conserved synteny at the *Or42a2*
1006 locus.
1007
1008 **Figure Supplement 7: Maxillary palp RNA seq of *S. pallida* and *S. flava Or*s.** The heatmap displays
1009 Log2[RPM+1] values of *Or*s expression in the maxillary palps of female (F) and male (M) *S. flava* and
1010 *S. pallida* (n=3/sex). Each column represents a replicate (e.g. *S. flava* F1: replicate #1 of female *S. flava*,
1011 *S. flava* M1: replicate #1 of male *S. flava*). Gray boxes indicate that the corresponding genes were
1012 unidentified in the genomes of the species. Only one copy of Or42a (Or42a2) is expressed in *S. pallida*,
1013 while *S. flava* expresses three copies. We confirmed the expression of homologs *Or71a* (expressed in
1014 OSNs of *D. melanogaster* pb1b), and of *Or33c/Or85e* and *Or46a* (expressed in OSNs of *D.*

1015 *melanogaster* pb2a and pb2b) in both *S. pallida* and *S. flava* maxillary palps. *Or85d* and *Or59c* were
1016 respectively expressed in *D. melanogaster* pb3a and pb3b OSNs but the homologs were unidentified in
1017 the genomes of *Scaptomyza* (Goldman-Huertas et al., 2015). Instead, *Or59a1, Or67a1, Or67a2,* and
1018 *OrN2a* were strongly expressed in OSNs of both *S. pallida* and *S. flava,* suggesting that these homologs
1019 may be expressed in pb3a or pb3b.

1020

1021 **Figure Supplement 8: Over-representation of pb1-like sensilla in mustard plant specialists.**
1022 Picture of single sensillum recording from *S. flava* maxillary palp sensilla (top left) and a representative
1023 anatomical mapping of *S. flava* palp sensilla (bottom left) obtained using diagnostic chemicals. Green:
1024 pb1-like, red: pb2-like, and magenta: pb3-like. Boxplots in the graph (right) represent the number of
1025 each sensilla type in *D. melanogaster* and the four *Scaptomyza* species (n=3 animals/species; see Figure
1026 Supplement 9 for individual maps). Maxillary palp pb1 sensilla are over-represented in *S. flava* and *S.*
1027 *montana*, the two mustard specialists.

1028

1029 **Figure Supplement 9: Location and percentages of the three different maxillary palp basiconic**
1030 **(pb) sensilla across species.** Classification of maxillary palp pb sensilla using single sensillum
1031 recordings and stimulation with diagnostic odorants. Data represents the proportion of pb1 and pb1-like
1032 (green), pb2 and pb2-like (red), and pb3 and pb3-like (magenta) in *D. melanogaster, S. hsui, S. pallida,*
1033 *S. flava,* and *S. montana*. The schematic positions of pb sensilla in each of the three replicates (R1, R2,
1034 and R3) from each species are shown on the right. The total number of sensilla identified in each animal
1035 is indicated between parentheses.

1036

1037 **Figure Supplement 10: Alignment of 1D and 3D structures of amino acids of Or42a. (A)** The 1D
1038 alignment of amino acids of *S. pallida* Or42a2, *S. flava* Or42a3, *S. flava* Or42a4, and *S. montana*
1039 Or42a2. Red arrowheads on top denote the sites where site-directed-mutagenesis was performed to
1040 generate the A181D S301P chimera. **(B)** The 3D structures of *S. flava* Or42a3, *S. flava* Or42a4, A181D
1041 S301P, and *S. montana* Or42a2 were predicted using AlphaFold2. The colors of the amino acids indicate
1042 the predicted local distance difference test (pLDDT) scores: blue (>90), cyan (>70), yellow (> 50), and
1043 orange (<50). We confirmed that the scores for these non-overlapping sites were above 70, indicating
1044 that the 3D predictions of these sites are reliable.

1045

1046 **Figure Supplement 11: Screening of candidate amino acids by AlphaFold2 3D prediction. (A)**
1047 Lateral view of the 3D structure of A181D S301P predicted by AlphaFold2 (left). *S. flava* Or42a3-
1048 derived amino acids are indicated in magenta, and the substitutions with *S. flava* Or42a4-derived amino
1049 acids are represented in green. The middle and right panels respectively display side and top views of
1050 alignment of the predicted structures of *S. flava* Or42a3, *S. flava* Or42a4, and A181D S301P. The
1051 extracellular region at S5 and S6 (red arrows) highlights the local structural differences between *S. flava*
1052 Or42a3 and Or42a4 where the A181D, S301P overlaps with the local structure of *S. flava* Or42a4. **(B)**
1053 The 3D predictions of *S. flava* Or42a3 (magenta), *S. flava* Or42a4 (green), and A181D S301P (cyan)
1054 were aligned using PyMol 2.5.3. Red rectangles highlight the sites of local structural variance between
1055 *S. flava* Or42a3 and Or42a4. The A181D S301P shows a closer alignment with Or42a4. S5' and S6' are
1056 enlarged views of S5 and S6, respectively. **(C)** The enlarged views of S5 and S6 in the alignment of 3D
1057 predictions of *S. flava* Or42a3 (magenta), *S. flava* Or42a4 (green), and *S. montana* Or42a2 (cyan). **(D)**
1058 The 3D alignment of *S. flava* Or42a3 and *S. montana* Or42a2 predicted by AlphaFold2. The root mean
1059 square deviation (RMSD) is visualized with a color gradient.

1060

1061 **Figure Supplement 12: Responses of OSNs expressing homozygous Or42a to stimulation with**
1062 **butyl isothiocyanate and γ-hexalactone.** Left: responses of OSNs expressing homozygous *S. flava*
1063 Or42a3, *S. flava* Or42a4, or A181D S307P (*UAS-Or42a; Or67d* ^{Gal4}) to stimulation with butyl
1064 isothiocyanate (BITC, white) and γ-hexalactone (grey) (n=16-30 from 5-10 animals). Right: ratio
1065 between responses to BITC and the sum of the responses evoked by stimulation with BITC and γ-
1066 hexalactone. Kruskal-Wallis followed by Dunn's multiple comparisons, *$p<0.05$.

1067

1068 **Figure Supplement 13: A model for the evolution of Or42a in *S. flava, S. montana* and *S. pallida*.**
1069 The evolution of Or42a begins with a shift in the ligand specificity of an ancestral Or42a (a), which was
1070 tuned to fruit-borne odors such as γ-hexalactone and limited ITCs (i.e. AITC), and later it broadened to
1071 detect a wider range of ITCs (b). Subsequent gene triplication of *S. flava Or42a* resulted in three
1072 paralogous genes (c: *S. flava Or42a2, S. flava Or42a3,* and *S. flava Or42a4*). The lineage leading to *S.*
1073 *flava* Or42a2 and *S. flava* Or42a4 experienced a reduction in sensitivity to γ-hexalactone (arrow pointing

1074 to the right in the bottom rightmost panel), while both *S. flava* Or42a3 and *S. montana* Or42a2 retained
1075 sensitivity to γ-hexalactone.

1076

1077 **SUPPLEMENTARY MATERIAL AND METHODS:**

1078 **Dilution series**

1079 *Trans*-2-hexenal, AITC, butyl ITC, isobutyl ITC, *sec*-butyl ITC, and ethyl butyrate were diluted in
1080 mineral oil, and γ-hexalactone was diluted in DMSO to concentrations ranging from 10^{-5} to 10^{-2} vol/vol.
1081 Half maximal effective concentration (EC50) was generated by GraphPad Prism v10.2.1.

1082 **Construction of the Or42a gene tree**

1083 The amino acid sequences of *D. melanogaster Or42a,* and *S. flava Or42a1, S. flava Or42a2, S. flava*
1084 *Or42a3,* and *S. flava Or42a4* were obtained from Flybase (2024_01), and Goldman-Huertas et al.
1085 (2015). Blast searches were conducted to annotate *S. hsui Or42a1, S. pallida Or42a1, S. graminum*
1086 *Or42a1, S. graminum Or42a2, S. montana Or42a1, S. montana Or42a2, S. flava Or42a1, S. hsui*
1087 *Or42a2,* and *S. pallida Or42a2,* using *S. flava Or42a1* and *S. flava Or42a2* as query against the
1088 genomes of *S. hsui* (ASM1815282v1), *S. pallida* (ASM1815296v1), *S. graminum* (ASM1890183v1),
1089 and *S. montana* (ASM1890430v1). Amino acid sequences of *S. hsui Or42a1, S. pallida Or42a1, S.*
1090 *gramina Or42a1, S. graminum Or42a2, S. montana Or42a1, S. montana Or42a, S. flava Or42a1, S.*
1091 *flava Or42a2, S. flava Or42a3, S. flava Or42a4, S. hsui Or42a2, S. pallida Or42a2* (Katoh and Standley
1092 2013), and *D. melanogaster Or42a* were aligned by MAFFT v7.511 with JTT as scoring matrix for
1093 amino acid sequences with L-INS-i strategy. Maximum-likelihood gene tree with 1000 bootstrap cycles
1094 using the above sequences were constructed with RAxML (v8.2.19) (Stamatakis 2014). GAMMA model
1095 of rate heterogeneity was applied. CDS and alignment of *Or42a* are included in Supplementary files 12
1096 and 13, respectively.

1097 **Alignment of *S. flava Or42a3* and *Or42a4*, and *S. montana Or42a2* using AlphaFold2 3D structural**
1098 **prediction**

1099 CDSs of *S. flava Or42a3*, *S. flava Or42a4,* and *S. montana Or42a2* were used as inputs into ColabFold
1100 (Jumper et al. 2021; Mirdita et al. 2022). The output models ranked first (rank1) were selected,
1101 visualized, and 3D-aligned by using PyMol2.5.3.

1102

1103 **Syntenic analysis using DiGAlign**

1104 To analyze synteny around the *Or42a2*-*Or42a4* loci, we extracted genomic regions spanning a total of
1105 30kb (15kb upstream and 15kb downstream of the *Or42a2*s start site) from the genomes of *S. montana*
1106 (ASM1890430v1), *S. pallida* (ASM1815296v1), and *S. hsui* (ASM1815282v1). For *S. flava* (sfla_v2),
1107 we extracted a 60,199 bp region, encompassing 15kb upstream of the *Or42a2* start site through 15kb
1108 downstream of the *Or42a4* start site (Kim et al. 2021; Peláez et al. 2023). For visualization purposes, the
1109 genomes of *S. montana, S. graminum,* and *S. pallida* were reverse-aligned. Synteny maps and dot plots
1110 were generated and visualized using DiGAlign (Nishimura et al. 2024).

1111

1112 **SUPPLEMENTARY FILES:**

1113 Supplementary file 1: Chemical list

1114 Supplementary file 2: Control-subtracted net number of spikes/sec and EC_{50} obtained from SSRs

1115 Supplementary file 3: Mobility assay data

1116 Supplementary file 4: Olfactory positional assay data and trap assay data

1117 Supplementary file 5: Consumption assay data

1118 Supplementary file 6: Expression intensity from maxillary palp RNA-seq

1119 Supplementary file 7: OSNs counts from RNA fluorescent in situ hybridization

1120 Supplementary file 8: Primer list

1121 Supplementary file 9: AlphaFold2 (Colabfold) prediction in pdb format

1122 Supplementary file 10: Pb sensilla counts from single sensillum recording experiments

1123 Supplementary file 11: CDS of *Or42a* homologs in fasta format

1124 Supplementary file 12: Alignment of *Or42a* homologs in fasta format

1125

1126 **DATA AVAILABILITY:**

1127 The data presented in this study are available on request from the corresponding authors.

1128

1129 **REFERENCES**

1130 Aguilar JM, Gloss AD, Suzuki HC, Verster KI, Singhal M, Hoff J, Grebenok R, Nabity PD, Behmer ST,
1131 Whiteman NK. 2024. Insights into the evolution of herbivory from a leaf‐mining fly.
1132 *Ecosphere* [Internet] 15. Available from:
1133 https://esajournals.onlinelibrary.wiley.com/doi/10.1002/ecs2.4764

1134 Ahuja I, Rohloff J, Bones AM. 2010. Defence mechanisms of Brassicaceae: implications for plant-insect
1135 interactions and potential for integrated pest management. A review. *Agron. Sustain. Dev.*
1136 30:311–348.

1137 Al-Anzi B, Tracey WD Jr, Benzer S. 2006. Response of Drosophila to wasabi is mediated by painless,
1138 the fly homolog of mammalian TRPA1/ANKTM1. *Curr. Biol.* 16:1034–1040.

1139 Anders S, Pyl PT, Huber W. 2015. HTSeq--a Python framework to work with high-throughput
1140 sequencing data. *Bioinformatics* 31:166–169.

1141 Auer TO, Khallaf MA, Silbering AF, Zappia G, Ellis K, Álvarez-Ocaña R, Arguello JR, Hansson BS,
1142 Jefferis GSXE, Caron SJC, et al. 2020. Olfactory receptor and circuit evolution promote host
1143 specialization. *Nature* 579:402–408.

1144 Becher PG, Bengtsson M, Hansson BS, Witzgall P. 2010. Flying the fly: long-range flight behavior of
1145 Drosophila melanogaster to attractive odors. *J. Chem. Ecol.* 36:599–607.

1146 Bell L, Oloyede OO, Lignou S, Wagstaff C, Methven L. 2018. Taste and flavor perceptions of
1147 glucosinolates, isothiocyanates, and related compounds. *Mol. Nutr. Food Res.* 62:e1700990.

1148 Benton R, Himmel NJ. 2023. Structural screens identify candidate human homologs of insect
1149 chemoreceptors and cryptic Drosophila gustatory receptor-like proteins. *Elife* 12:e85537.

1150 Bernays E, Chapman R. 1987. The evolution of deterrent responses in plant-feeding insects. In:
1151 Proceedings in Life Sciences. New York, NY: Springer New York. p. 159–173.

1152 Bischof J, Maeda RK, Hediger M, Karch F, Basler K. 2007. An optimized transgenesis system for
1153 Drosophila using germ-line-specific phiC31 integrases. *Proc. Natl. Acad. Sci. U. S. A.* 104:3312–
1154 3317.

1155 de Bruyne M, Clyne PJ, Carlson JR. 1999. Odor coding in a model olfactory organ: the Drosophila
1156 maxillary palp. *J. Neurosci.* 19:4520–4532.

1157 Butterwick JA, Del Mármol J, Kim KH, Kahlson MA, Rogow JA, Walz T, Ruta V. 2018. Cryo-EM
1158 structure of the insect olfactory receptor Orco. *Nature* 560:447–452.

1159 Chen S, Zhou Y, Chen Y, Gu J. 2018. fastp: an ultra-fast all-in-one FASTQ preprocessor.
1160 *Bioinformatics* 34:i884–i890.

1161 Chen Y-CD, Dahanukar A. 2020. Recent advances in the genetic basis of taste detection in Drosophila.
1162 *Cell. Mol. Life Sci.* 77:1087–1101.

1163 Chou PY, Fasman GD. 1978. Prediction of the secondary structure of proteins from their amino acid
1164 sequence. *Adv. Enzymol. Relat. Areas Mol. Biol.* 47:45–148.

1165 Couto A, Alenius M, Dickson BJ. 2005. Molecular, anatomical, and functional organization of the
1166 Drosophila olfactory system. *Curr. Biol.* 15:1535–1547.

1167 Crowley-Gall A, Date P, Han C, Rhodes N, Andolfatto P, Layne JE, Rollmann SM. 2016. Population
1168 differences in olfaction accompany host shift in Drosophila mojavensis. *Proc. Biol. Sci.*
1169 [Internet] 283. Available from: https://www.ncbi.nlm.nih.gov/pmc/articles/PMC5013806/

1170 Cuellar-Nuñez ML, Luzardo-Ocampo I, Lee-Martínez S, Larrauri-Rodríguez M, Zaldívar-Lelo de
1171 Larrea G, Pérez-Serrano RM, Camacho-Calderón N. 2022. Isothiocyanate-Rich Extracts from
1172 Cauliflower (Brassica oleracea Var. Botrytis) and Radish (Raphanus sativus) Inhibited Metabolic
1173 Activity and Induced ROS in Selected Human HCT116 and HT-29 Colorectal Cancer Cells. *Int.*
1174 *J. Environ. Res. Public Health* [Internet] 19. Available from:
1175 http://dx.doi.org/10.3390/ijerph192214919

1176 Dekker T, Ibba I, Siju KP, Stensmyr MC, Hansson BS. 2006. Olfactory shifts parallel superspecialism
1177 for toxic fruit in Drosophila melanogaster sibling, D. sechellia. *Curr. Biol.* 16:101–109.

1178 Del Mármol J, Yedlin MA, Ruta V. 2021. The structural basis of odorant recognition in insect olfactory
1179 receptors. *Nature* 597:126–131.

1180 Dobin A, Davis CA, Schlesinger F, Drenkow J, Zaleski C, Jha S, Batut P, Chaisson M, Gingeras TR.
1181 2013. STAR: ultrafast universal RNA-seq aligner. *Bioinformatics* 29:15–21.

1182 Dobler S, Dalla S, Wagschal V, Agrawal AA. 2012. Community-wide convergent evolution in insect
1183 adaptation to toxic cardenolides by substitutions in the Na,K-ATPase. *Proc. Natl. Acad. Sci. U.*
1184 *S. A.* 109:13040–13045.

1185 Dobritsa AA, van der Goes van Naters W, Warr CG, Steinbrecht RA, Carlson JR. 2003. Integrating the
1186 molecular and cellular basis of odor coding in the Drosophila antenna. *Neuron* 37:827–841.

1187 Dweck HK, Ebrahim SA, Khallaf MA, Koenig C, Farhan A, Stieber R, Weißflog J, Svatoš A, Grosse-
1188 Wilde E, Knaden M, et al. 2016. Olfactory channels associated with the Drosophila maxillary
1189 palp mediate short- and long-range attraction. *Elife* [Internet] 5. Available from:
1190 https://www.ncbi.nlm.nih.gov/pmc/articles/PMC4927298/

1191 Dweck HKM, Carlson JR. 2020. Molecular logic and evolution of bitter taste in Drosophila. *Curr. Biol.*
1192 30:17-30.e3.

1193 Ferreiro MJ, Pérez C, Marchesano M, Ruiz S, Caputi A, Aguilera P, Barrio R, Cantera R. 2017.
1194 Drosophila melanogaster white mutant w1118 undergo retinal degeneration. *Front. Neurosci.*
1195 11:732.

1196 Gloss AD, Brachi B, Feldmann MJ, Groen SC, Bartoli C, Gouzy J, LaPlante ER, Meyer CG, Pyon HS,
1197 Rogan SC, et al. 2017. Genetic variants affecting plant size and chemical defenses jointly shape
1198 herbivory in*Arabidopsis*. *bioRxiv* [Internet]:156299. Available from:
1199 https://www.biorxiv.org/content/10.1101/156299v1

1200 Goldman-Huertas B, Mitchell RF, Lapoint RT, Faucher CP, Hildebrand JG, Whiteman NK. 2015.
1201 Evolution of herbivory in Drosophilidae linked to loss of behaviors, antennal responses, odorant
1202 receptors, and ancestral diet. *Proceedings of the National Academy of Sciences* 112:3026–3031.

1203 Gonzalez F, Witzgall P, Walker WB. 2016. Protocol for heterologous expression of insect odourant
1204 receptors in Drosophila. *Front. Ecol. Evol.* [Internet] 4. Available from:
1205 https://www.frontiersin.org/journals/ecology-and-
1206 evolution/articles/10.3389/fevo.2016.00024/full

1207 Hashimoto Y, Yoshimura M, Huang R-N. 2019. Wasabi versus red imported fire ants: preliminary test
1208 of repellency of microencapsulated allyl isothiocyanate against Solenopsis invicta
1209 (Hymenoptera: Formicidae) using bait traps in Taiwan. *Appl. Entomol. Zool. (Jpn.)* 54:193–196.

1210 Haverkamp A, Hansson BS, Knaden M. 2018. Combinatorial codes and labeled lines: How insects use
1211 olfactory cues to find and judge food, mates, and oviposition sites in complex environments.
1212 *Front. Physiol.* 9:49.

1213 Himmel NJ, Moi D, Benton R. 2023. Remote homolog detection places insect chemoreceptors in a
1214 cryptic protein superfamily spanning the tree of life. *Curr. Biol.* 33:5023-5033.e4.

1215 Hopkins RJ, van Dam NM, van Loon JJA. 2009. Role of glucosinolates in insect-plant relationships and
1216 multitrophic interactions. *Annu. Rev. Entomol.* 54:57–83.

1217 Ibanez S, Gallet C, Després L. 2012. Plant insecticidal toxins in ecological networks. *Toxins (Basel)*
1218 4:228–243.

1219 Iorio R, Celenza G, Petricca S. 2022. Multi-target effects of ß-caryophyllene and carnosic acid at the
1220 Crossroads of mitochondrial dysfunction and neurodegeneration: From oxidative stress to
1221 microglia-mediated neuroinflammation. *Antioxidants (Basel)* 11:1199.

1222 Jumper J, Evans R, Pritzel A, Green T, Figurnov M, Ronneberger O, Tunyasuvunakool K, Bates R,
1223 Žídek A, Potapenko A, et al. 2021. Highly accurate protein structure prediction with AlphaFold.
1224 *Nature* 596:583–589.

1225 Kang K, Pulver SR, Panzano VC, Chang EC, Griffith LC, Theobald DL, Garrity PA. 2010. Analysis of
1226 Drosophila TRPA1 reveals an ancient origin for human chemical nociception. *Nature* 464:597–
1227 600.

1228 Katoh K, Standley DM. 2013. MAFFT multiple sequence alignment software version 7: improvements
1229 in performance and usability. *Mol. Biol. Evol.* 30:772–780.

1230 Kim BY, Wang JR, Miller DE, Barmina O, Delaney E, Thompson A, Comeault AA, Peede D,
1231 D'Agostino ERR, Pelaez J, et al. 2021. Highly contiguous assemblies of 101 drosophilid
1232 genomes. *Elife* [Internet] 10. Available from: https://pubmed.ncbi.nlm.nih.gov/34279216/

1233 Kim SH, Lee Y, Akitake B, Woodward OM, Guggino WB, Montell C. 2010. *Drosophila* TRPA1
1234 channel mediates chemical avoidance in gustatory receptor neurons. *Proceedings of the National*
1235 *Academy of Sciences* 107:8440–8445.

1236 Kurtovic A, Widmer A, Dickson BJ. 2007. A single class of olfactory neurons mediates behavioural
1237 responses to a Drosophila sex pheromone. *Nature* 446:542–546.

1238 Larsson MC, Domingos AI, Jones WD, Chiappe ME, Amrein H, Vosshall LB. 2004. Or83b encodes a
1239 broadly expressed odorant receptor essential for Drosophila olfaction. *Neuron* 43:703–714.

1240 Levitt M. 1978. Conformational preferences of amino acids in globular proteins. *Biochemistry* 17:4277–
1241 4285.

1242 Lichtenstein EP, Morgan DG, Mueller CH. 1964. Insecticides in Nature, Naturally Occurring
1243 Insecticides in Cruciferous Crops. *J. Agric. Food Chem.* 12:158–161.

1244 Lin C-C, Prokop-Prigge KA, Preti G, Potter CJ. 2015. Food odors trigger Drosophila males to deposit a
1245 pheromone that guides aggregation and female oviposition decisions. *Elife* 4:e08688.

1246 Linz J, Baschwitz A, Strutz A, Dweck HKM, Sachse S, Hansson BS, Stensmyr MC. 2013. Host plant-
1247 driven sensory specialization in Drosophila erecta. *Proc. Biol. Sci.* 280:20130626.

1248 Liu X-L, Zhang J, Yan Q, Miao C-L, Han W-K, Hou W, Yang K, Hansson BS, Peng Y-C, Guo J-M, et
1249 al. 2020. The molecular basis of host selection in a Crucifer-specialized moth. *Curr. Biol.*
1250 30:4476-4482.e5.

1251 MacLeod AJ, MacLeod G, Reader G. 1989. Evidence for the occurrence of butyl- and
1252 isobutylglucosinolates in seeds of Brassica oleracea. *Phytochemistry* 28:1405–1407.

1253 Mandel SJ, Shoaf ML, Braco JT, Silver WL, Johnson EC. 2018. Behavioral aversion to AITC requires
1254 both painless and dTRPA1 in Drosophila. *Front. Neural Circuits* 12:45.

1255 Mantel N. 1966. Evaluation of survival data and two new rank order statistics arising in its
1256 consideration. *Cancer Chemother. Rep.* 50:163–170.

1257 Mariani V, Biasini M, Barbato A, Schwede T. 2013. lDDT: a local superposition-free score for
1258 comparing protein structures and models using distance difference tests. *Bioinformatics*
1259 29:2722–2728.

1260 Martin NA. 2004. History of an invader,Scaptomyza flava(fallen, 1823) (Diptera: Drosophilidae). *N. Z.*
1261 *J. Zool.* 31:27–32.

1262 Matsunaga T, Reisenman CE, Goldman-Huertas B, Brand P, Miao K, Suzuki HC, Verster KI, Ramírez
1263 SR, Whiteman NK. 2021. Evolution of Olfactory Receptors Tuned to Mustard Oils in
1264 Herbivorous Drosophilidae. *Mol. Biol. Evol.* 39:msab362.

1265 Mirdita M, Schütze K, Moriwaki Y, Heo L, Ovchinnikov S, Steinegger M. 2022. ColabFold: making
1266 protein folding accessible to all. *Nat. Methods* 19:679–682.

1267 Mithöfer A, Boland W. 2012. Plant defense against herbivores: chemical aspects. *Annu. Rev. Plant Biol.*
1268 63:431–450.

1269 Nishimura Y, Yamada K, Okazaki Y, Ogata H. 2024. DiGAlign: Versatile and interactive visualization
1270 of sequence alignment for comparative genomics. *Microbes Environ.* 39:ME23061.

1271 Noge K, Becerra JX. 2015. 4-Oxo-(E)-2-hexenal produced by Heteroptera induces permanent
1272 locomotive impairment in crickets that correlates with free thiol depletion. *FEBS Open Bio*
1273 5:319–324.

1274 Oh SM, Jeong K, Seo JT, Moon SJ. 2021. Multisensory interactions regulate feeding behavior in
1275 Drosophila. *Proc. Natl. Acad. Sci. U. S. A.* 118:e2004523118.

1276 Orre GUS, Wratten SD, Jonsson M, Hale RJ. 2010. Effects of an herbivore-induced plant volatile on
1277 arthropods from three trophic levels in brassicas. *Biol. Control* 53:62–67.

1278 Peláez JN, Gloss AD, Goldman-Huertas B, Kim B, Lapoint RT, Pimentel-Solorio G, Verster KI, Aguilar
1279 JM, Nelson Dittrich AC, Singhal M, et al. 2023. Evolution of chemosensory and detoxification
1280 gene families across herbivorous Drosophilidae. *G3* [Internet] 13. Available from:
1281 http://dx.doi.org/10.1093/g3journal/jkad133

1282 Peláez JN, Gloss AD, Ray JF, Chaturvedi S, Haji D, Charboneau JLM, Verster KI, Whiteman NK.
1283 2022. Evolution and genomic basis of the plant-penetrating ovipositor: a key morphological trait
1284 in herbivorous Drosophilidae. *Proc. Biol. Sci.* 289:20221938.

1285 Rambaut A. 2009. FigTree, version 1.4.3. *Computer program distributed by the author, website:*
1286 *http://tree.bio.ed.ac.uk/software/figtree/[accessed January 4, 2011]* [Internet]. Available from:
1287 https://scholar.google.com/citations?view_op=view_citation&hl=en&citation_for_view=JiYPDf
1288 oAAAAJ:W5xh706n7nkC

1289 Ray A, van Naters W van der G, Shiraiwa T, Carlson JR. 2007. Mechanisms of odor receptor gene
1290 choice in Drosophila. *Neuron* 53:353–369.

1291 Reichstein T, von Euw J, Parsons JA, Rothschild M. 1968. Heart poisons in the monarch butterfly. Some
1292 aposematic butterflies obtain protection from cardenolides present in their food plants. *Science*
1293 161:861–866.

1294 Reisenman CE, Scott K. 2019. Food-derived volatiles enhance consumption in Drosophila
1295 melanogaster. *J. Exp. Biol.* 222:jeb202762.

1296 Scott K. 2018. Gustatory processing in Drosophila melanogaster. *Annu. Rev. Entomol.* 63:15–30.

1297 Semmelhack JL, Wang JW. 2009. Select Drosophila glomeruli mediate innate olfactory attraction and
1298 aversion. *Nature* 459:218–223.

1299 Shiraiwa T. 2008. Multimodal chemosensory integration through the maxillary palp in Drosophila. *PLoS*
1300 *One* 3:e2191.

1301 Southwood T. 1972. insect/plant relationship--an evolutionary perspective. Available from:
1302 https://www.semanticscholar.org/paper/insect%2Fplant-relationship--an-evolutionary-
1303 Southwood/635ed400c02b62dca75e90d7ee3e664383d480be

1304 Stamatakis A. 2014. RAxML version 8: a tool for phylogenetic analysis and post-analysis of large
1305 phylogenies. *Bioinformatics* 30:1312–1313.

1306 Stensmyr MC, Dweck HKM, Farhan A, Ibba I, Strutz A, Mukunda L, Linz J, Grabe V, Steck K,
1307 Lavista-Llanos S, et al. 2012. A conserved dedicated olfactory circuit for detecting harmful
1308 microbes in Drosophila. *Cell* 151:1345–1357.

1309 Takagi S, Sancer G, Abuin L, Stupski SD, Roman Arguello J, Prieto-Godino LL, Stern DL, Cruchet S,
1310 Álvarez-Ocaña R, Wienecke CFR, et al. 2024. Olfactory sensory neuron population expansions
1311 influence projection neuron adaptation and enhance odour tracking. *Nat. Commun.* 15:7041.

1312 Tocmo R, Veenstra JP, Huang Y, Johnson JJ. 2021. Covalent modification of proteins by plant-derived
1313 natural products: Proteomic approaches and biological impacts. *Proteomics* 21:e1900386.

1314 Wang Y, Qiu L, Wang Bing, Guan Z, Dong Z, Zhang J, Cao S, Yang L, Wang Bo, Gong Z, et al. 2024.
1315 Structural basis for odorant recognition of the insect odorant receptor OR-Orco heterocomplex.
1316 *Science* 384:1453–1460.

1317 War AR, Paulraj MG, Ahmad T, Buhroo AA, Hussain B, Ignacimuthu S, Sharma HC. 2012.
1318 Mechanisms of plant defense against insect herbivores. *Plant Signal. Behav.* 7:1306–1320.

1319 Winde I, Wittstock U. 2011. Insect herbivore counteradaptations to the plant glucosinolate-myrosinase
1320 system. *Phytochemistry* 72:1566–1575.

1321 Wu X, Huang H, Childs H, Wu Y, Yu L, Pehrsson PR. 2021. Glucosinolates in Brassica vegetables:
1322 Characterization and factors that influence distribution, content, and intake. *Annu. Rev. Food Sci.*
1323 *Technol.* 12:485–511.

1324 Yaffe PB, Power Coombs MR, Doucette CD, Walsh M, Hoskin DW. 2015. Piperine, an alkaloid from
1325 black pepper, inhibits growth of human colon cancer cells via G1 arrest and apoptosis triggered
1326 by endoplasmic reticulum stress: PIPERINE INHIBITS COLON CANCER CELL GROWTH.
1327 *Mol. Carcinog.* 54:1070–1085.

1328 Yao CA, Ignell R, Carlson JR. 2005. Chemosensory coding by neurons in the coeloconic sensilla of the
1329 Drosophila antenna. *J. Neurosci.* 25:8359–8367.

1330 Zhao J, Chen AQ, Ryu J, Del Mármol J. 2024. Structural basis of odor sensing by insect heteromeric
1331 odorant receptors. *Science* 384:1460–1467.

Supp. Figure 1

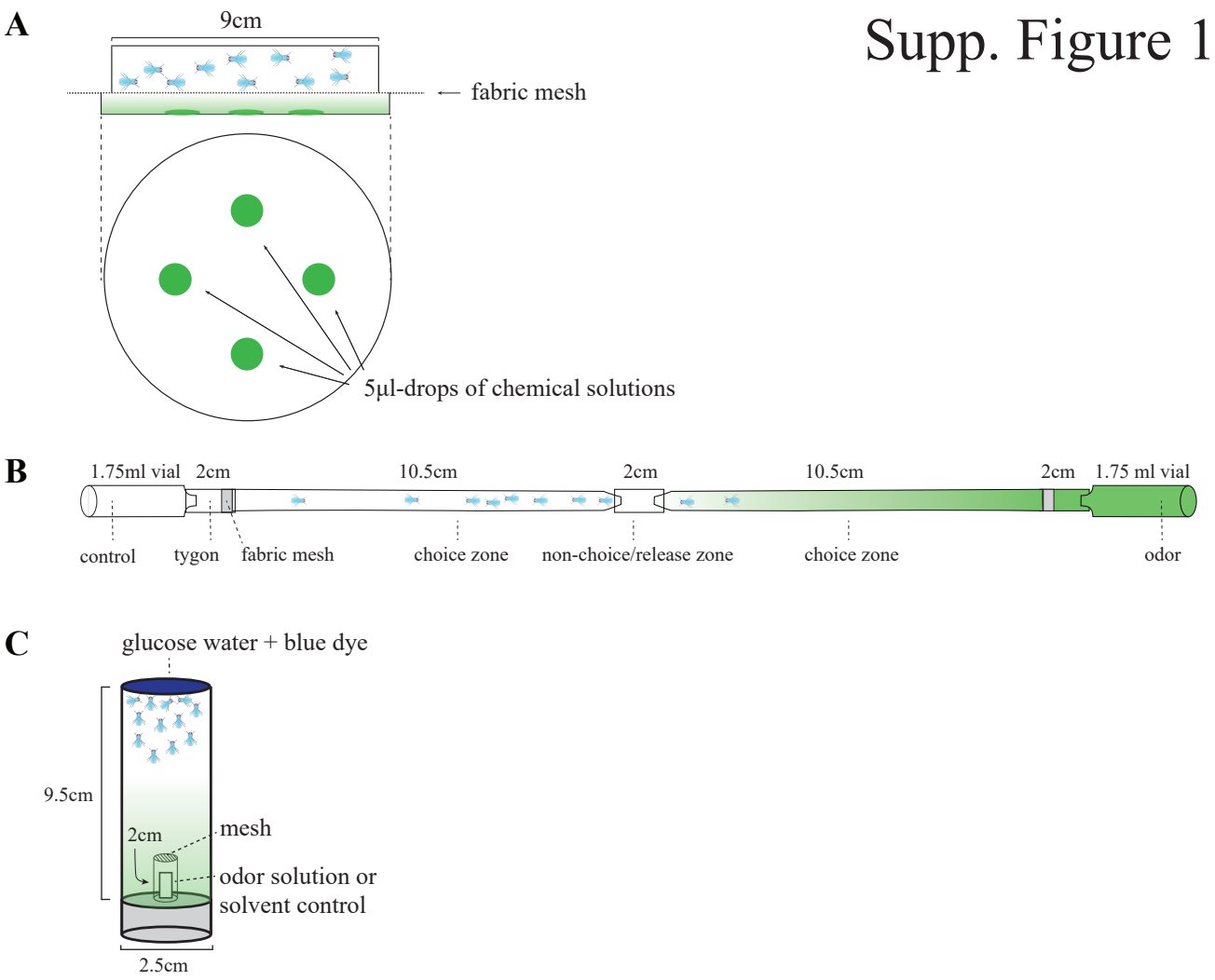

Supp. Figure 2

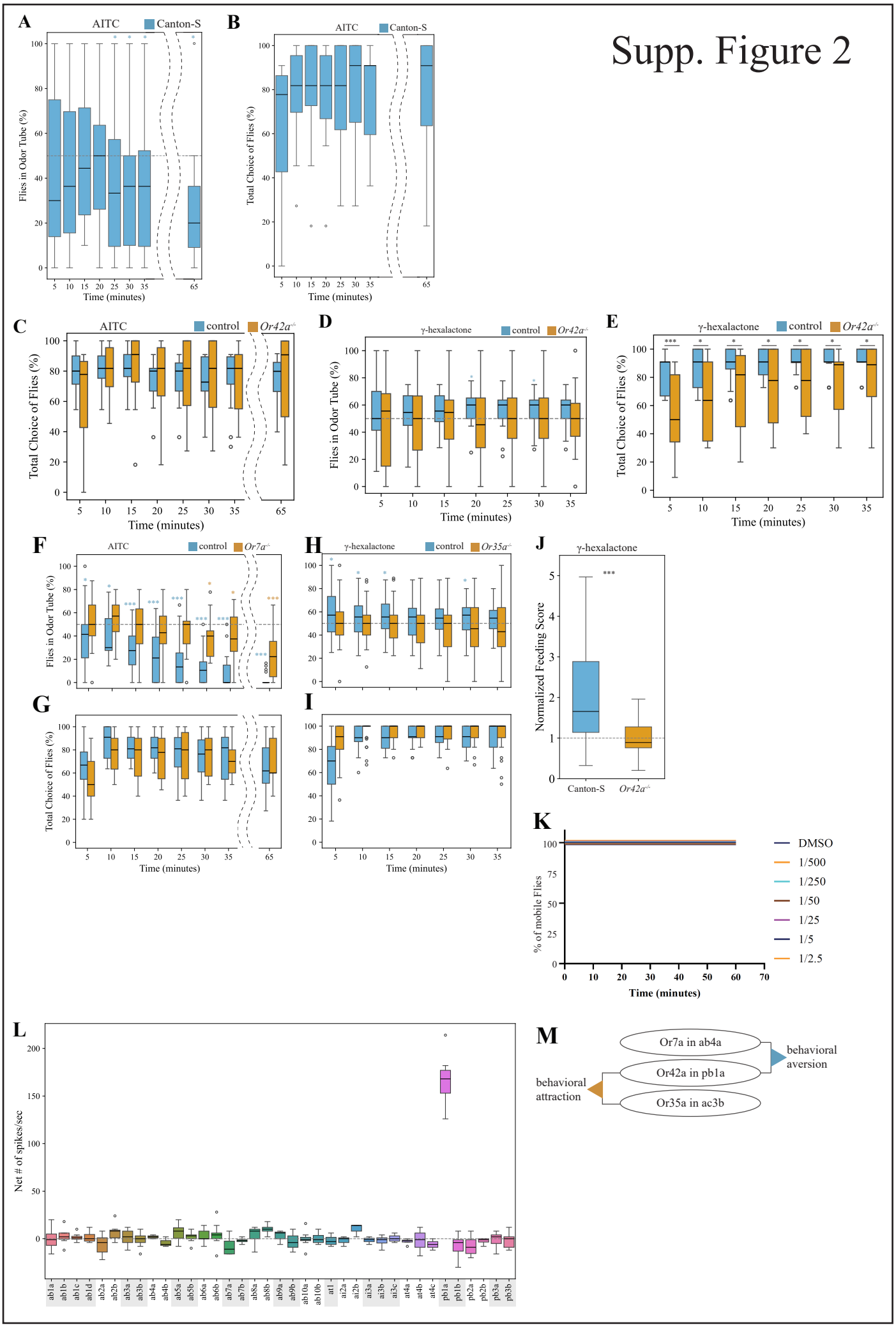

Supp. Figure 3

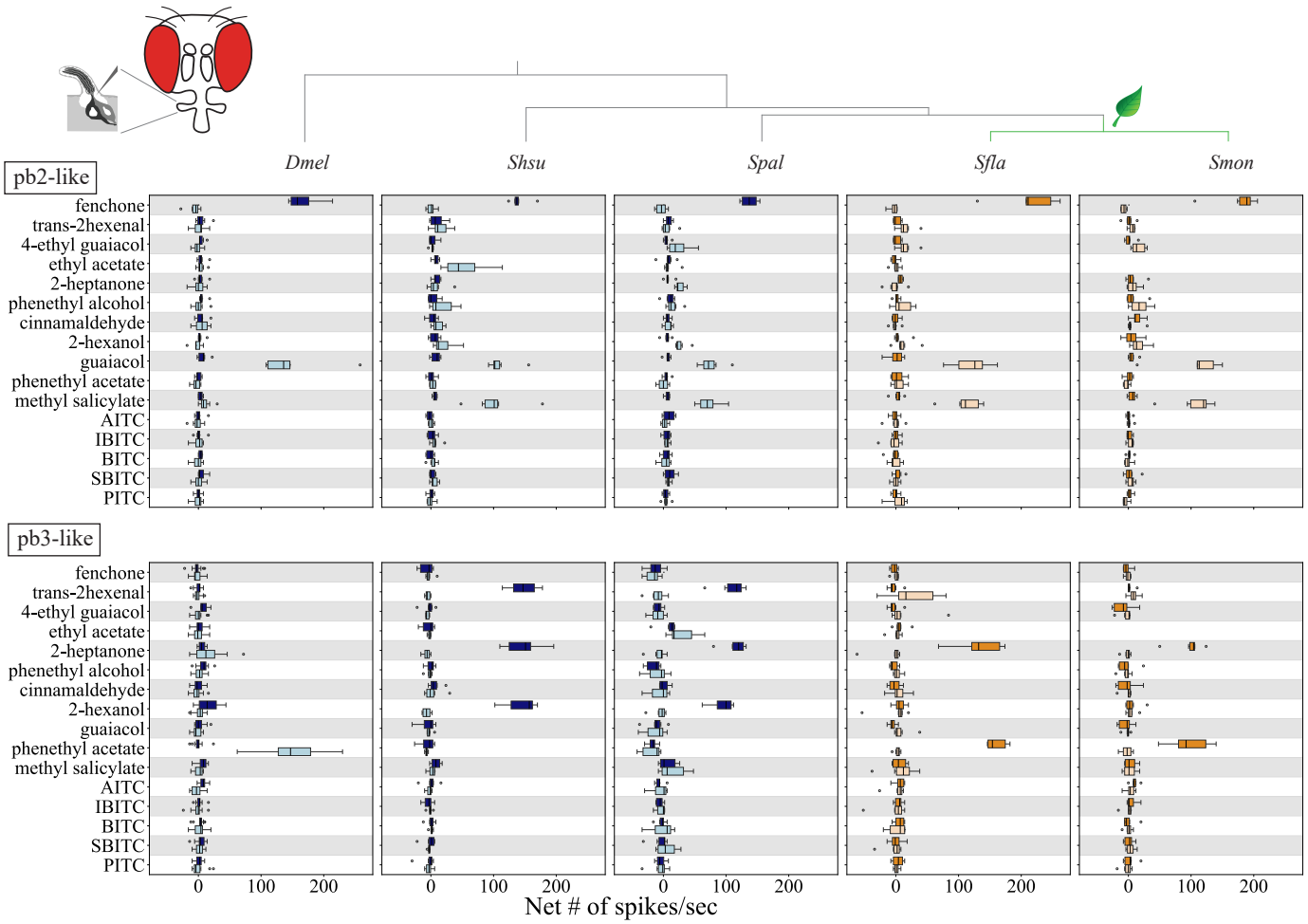

Supp.Figure 4

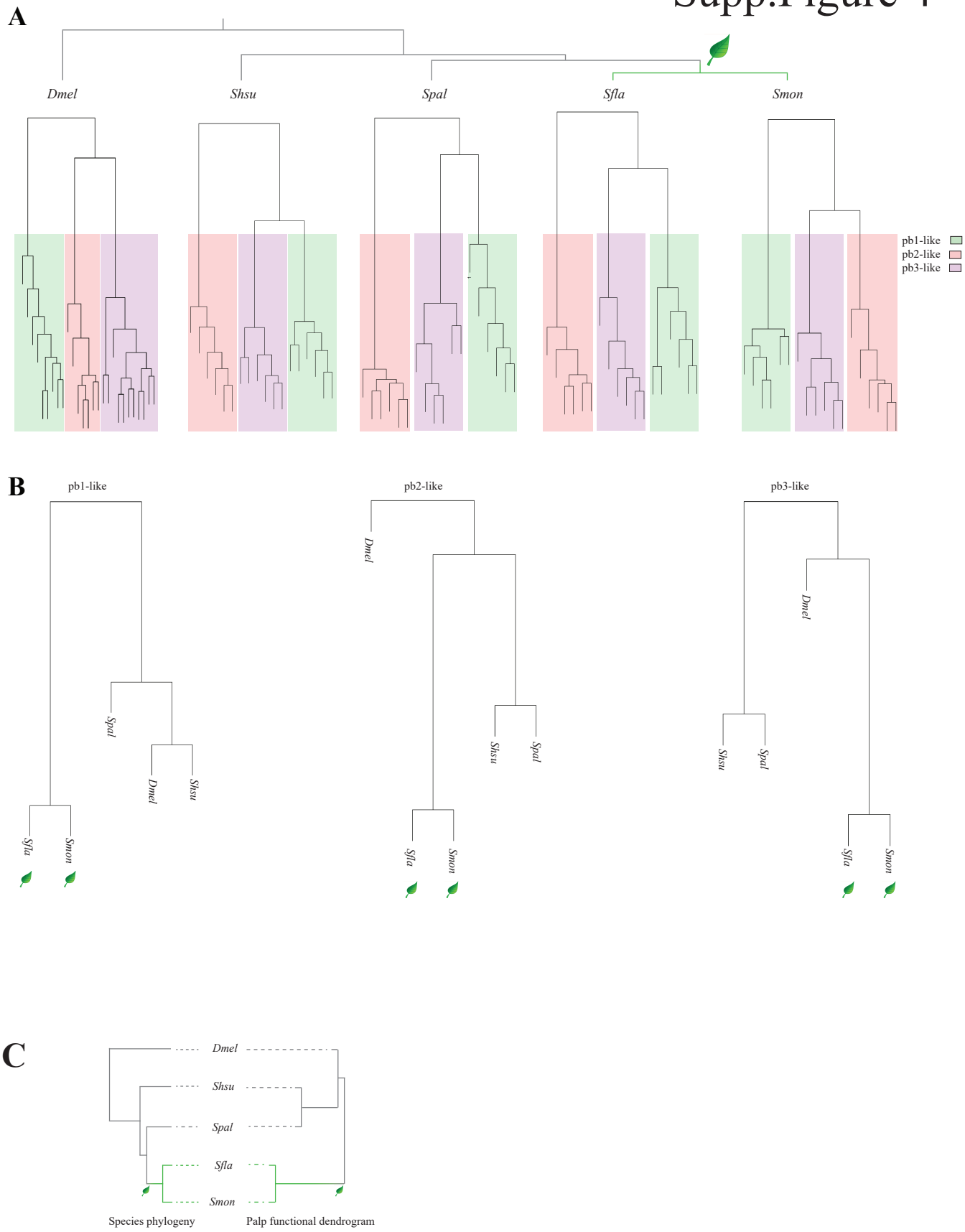

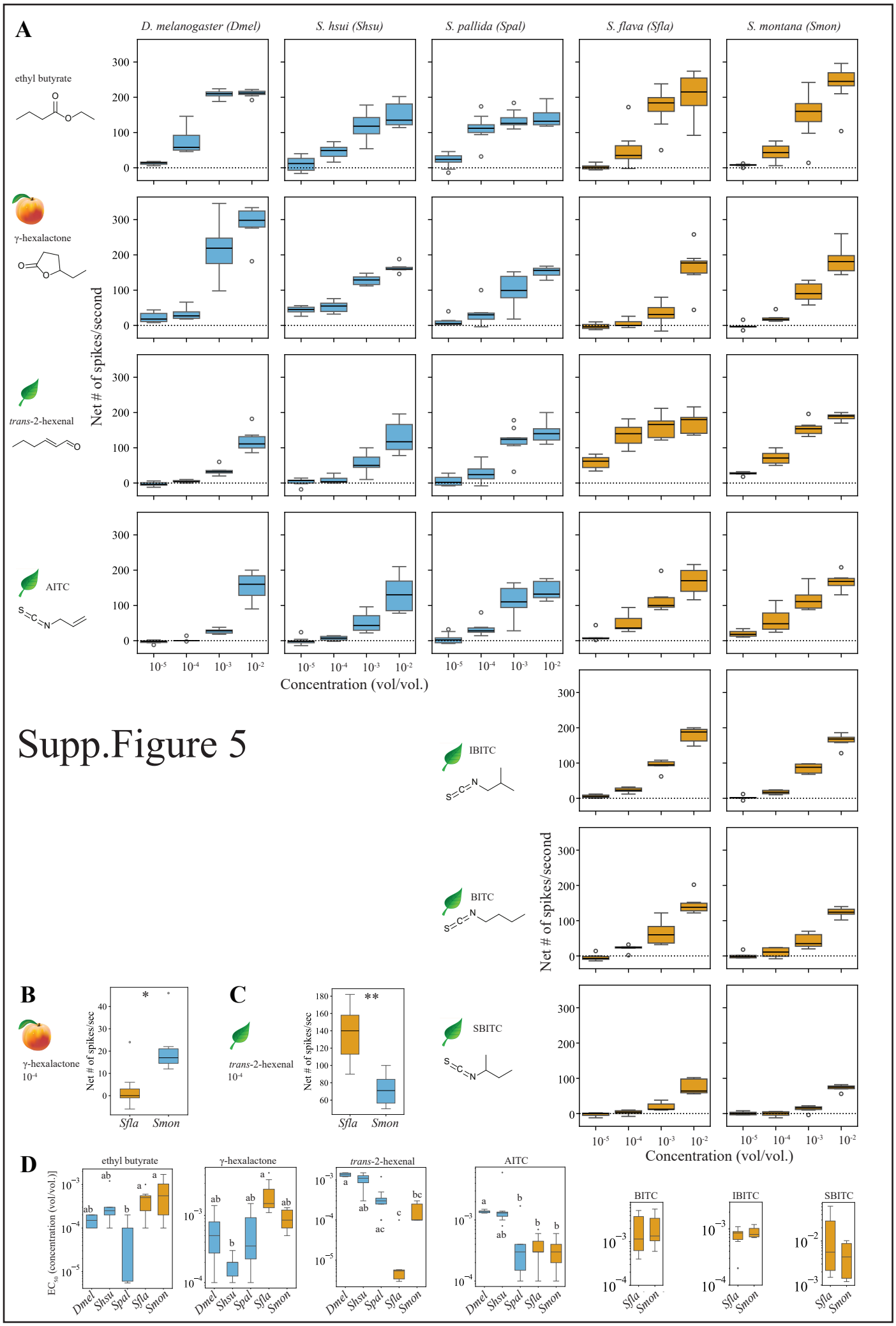

Supp.Figure 5

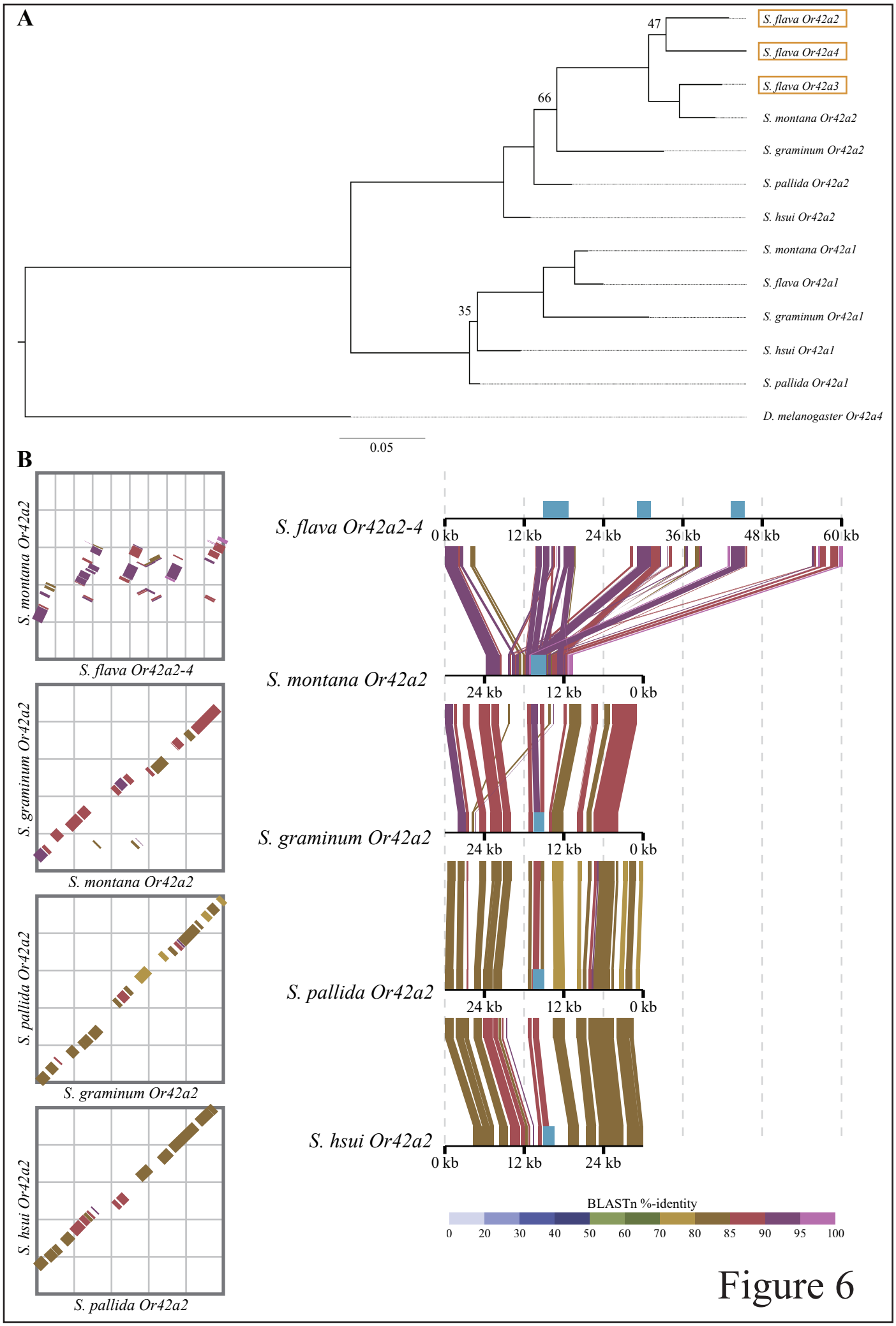
A
47
66
35
S. flava Or42a2
S. flava Or42a4
S. flava Or42a3
S. montana Or42a2
S. graminum Or42a2
S. pallida Or42a2
S. hsui Or42a2
S. montana Or42a1
S. flava Or42a1
S. graminum Or42a1
S. hsui Or42a1
S. pallida Or42a1
D. melanogaster Or42a4
0.05
B
S. montana Or42a2
S. flava Or42a2-4
S. graminum Or42a2
S. montana Or42a2
S. pallida Or42a2
S. graminum Or42a2
S. hsui Or42a2
S. pallida Or42a2
S. flava Or42a2-4
0 kb
12 kb
24 kb
36 kb
48 kb
60 kb
S. montana Or42a2
24 kb
12 kb
0 kb
S. graminum Or42a2
24 kb
12 kb
0 kb
S. pallida Or42a2
24 kb
12 kb
0 kb
S. hsui Or42a2
0 kb
12 kb
24 kb
BLASTn %-identity
0
20
30
40
50
60
70
80
85
90
95
100

Figure 6

Supp. Figure 7

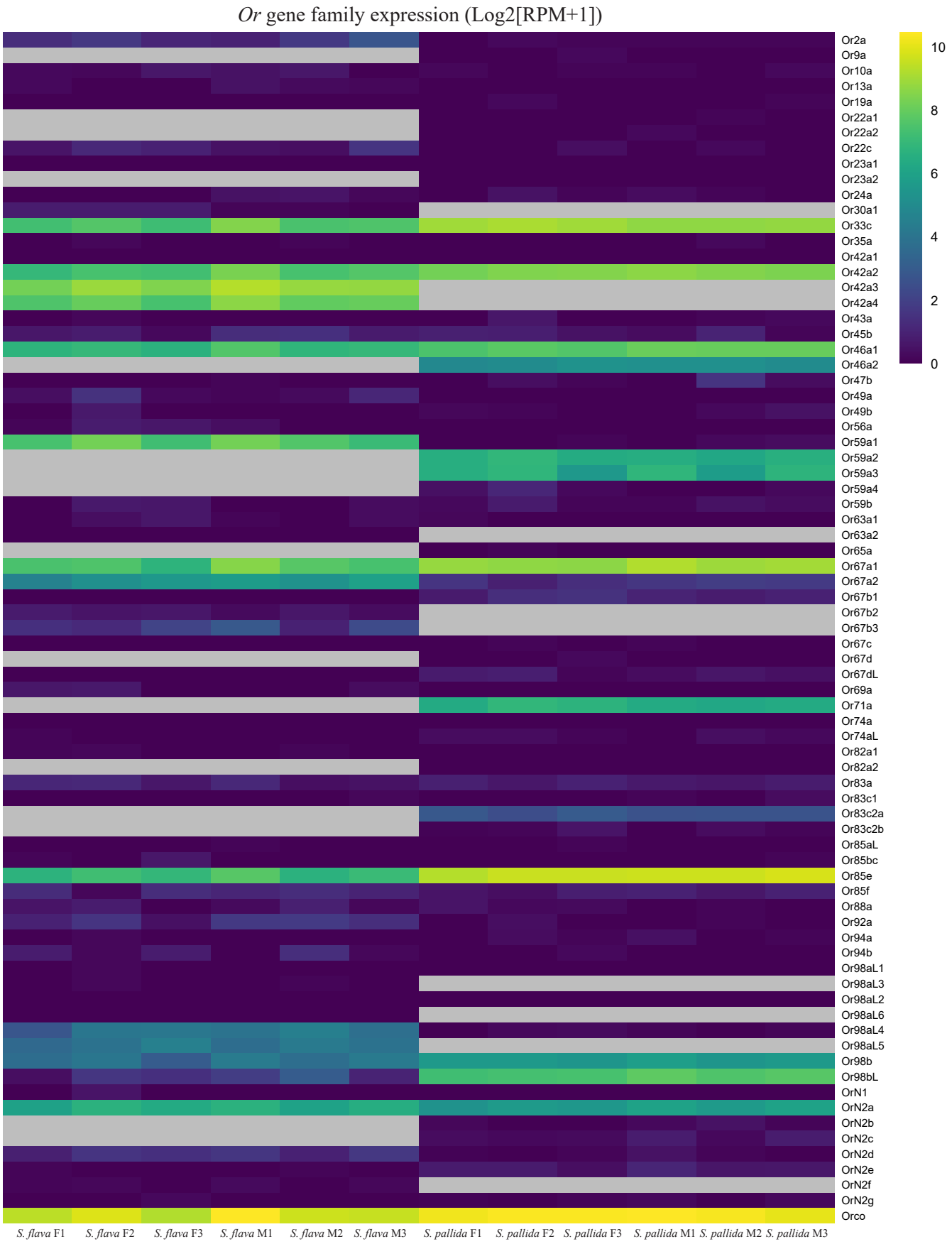

Supp. Figure 8

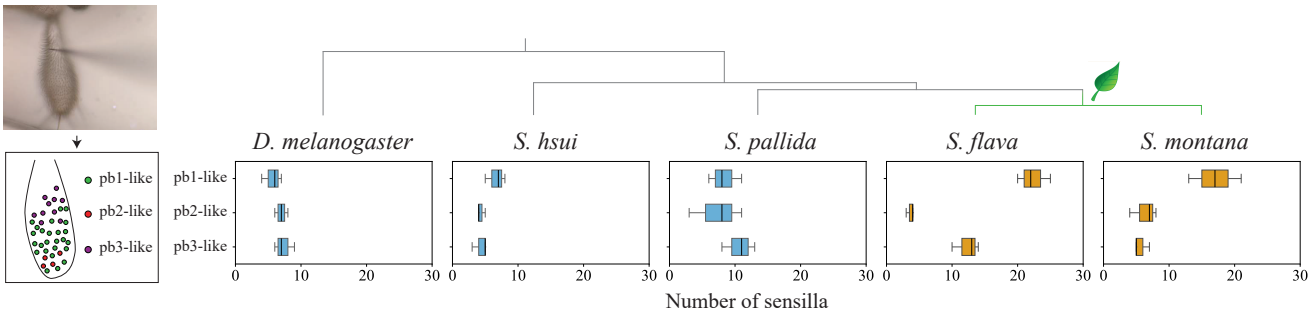

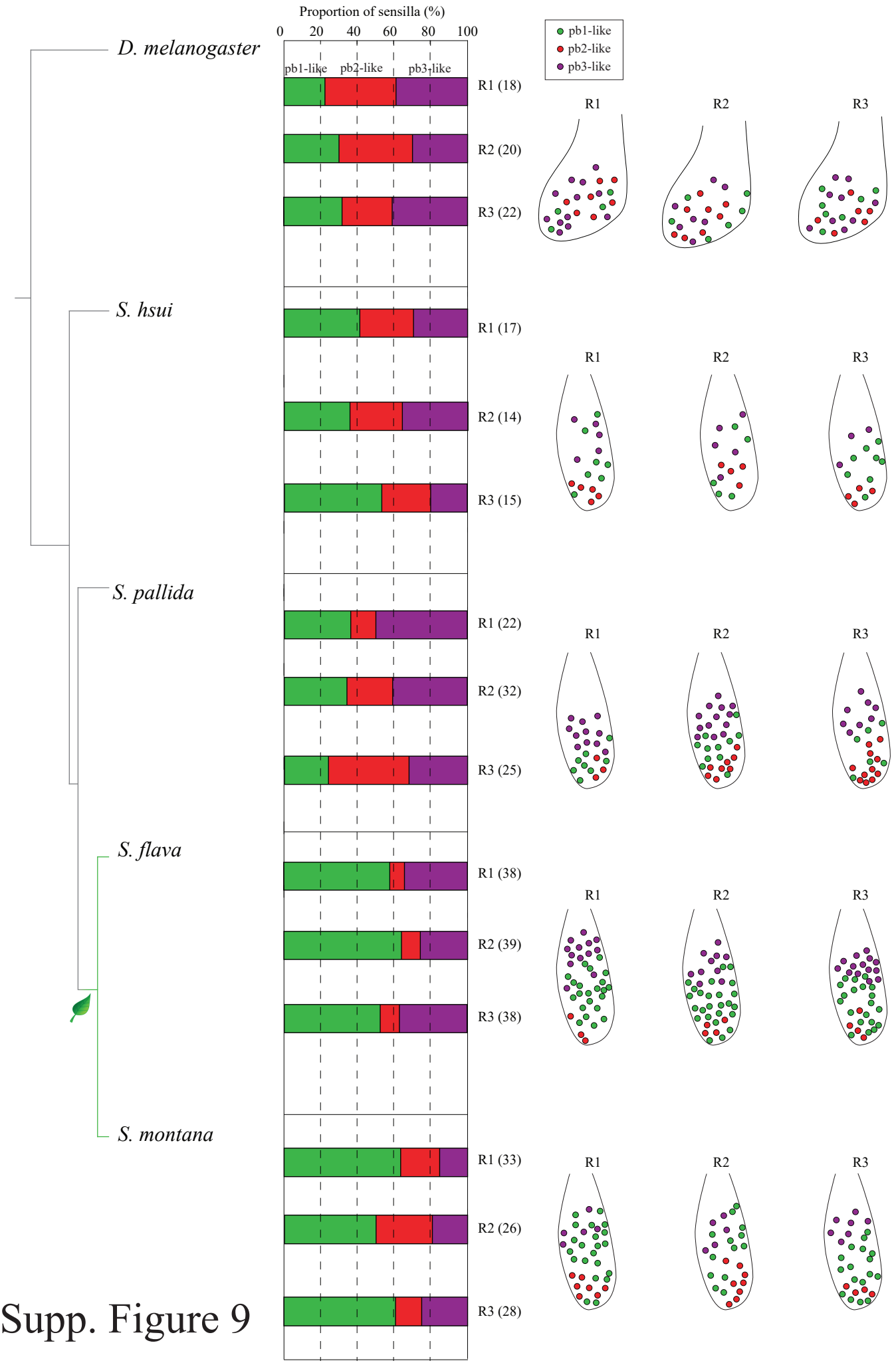

Supp. Figure 9

Supp. Figure 10

A

```
                 1         10        20        30        40        50
S. pallida Or42a2   MVLRKIFPSMYAKPDSAPPESRKATLYLLRCVFLMGIRTPPQRFFLIYCLWSFALN
S. flava Or42a3     MVLRNIFPSLYAKPDSAPPESRKATLYLLRCVFLMGIRTPPQRYFLIYCLWSFALN
S. flava Or42a4     MVLRNIFPSLYAKPDSAPPESRKATLYLLRCVFLMGIRTPPQRYFLIYCLWSFALN
S. montana Or42a2   MVLRNIFPSLYAKPDSAPPESRKATLYLLRCVFLMGIRTPPQRYFLIYCLWSFALN
                    60        70        80        90       100       110
S. pallida Or42a2   LSSTFYQPIGFMTGYISHLSEFSPGEFLTSLQVAFNAWSCSTKVIIVWVLVNRFDQ
S. flava Or42a3     MSSTFYQPIGFMLAYISHLSELSPGEFLTSLQVAFNTWACSTKVIIVWVLAKRFDE
S. flava Or42a4     LSSTFYQPIGFLMGYISHLSELSPGELLTSLQVAFNAWACSTKVIIVWVQVKRFDQ
S. montana Or42a2   MSSTFYQPIGFLMAYISHLSELSPGEFLTSLQVAFNTWSCSTKVIIVWVLAKRFDQ
                   120       130       140       150       160
S. pallida Or42a2   ANRILDKLDERLTKPSERARSHRAVASSNRIFFCFMTVYLLYATSTAVSAAAMGVP
S. flava Or42a3     ANLLLDKLDKQLKKPSDRARSHRAVANSNRFFFCFMTVNVLYATSAAVSAAAMGVP
S. flava Or42a4     ANLLLDKLDERLKKPSERARSHRAVANSNRIYFCFMTVYILYATSTAVSAAVMGVP
S. montana Or42a2   ANLLLDKLDERLTKPSERARSHRAVANSNRIFFCFMTVNVLYASSAAVSAAAMGVP
                   170       180       190       200       210       220
S. pallida Or42a2   SFQNYYPWLDWRASKWQFWLQSGLEYFAMLGACFQDVCVDCYPINFVLPLRAHMAN
S. flava Or42a3     SFQNYYPWLDWRASKWQFWLQSGLEYFAMLGACFQDACLDCFPINFVVPLRAHVAN
S. flava Or42a4     SFQNYYPWLDWRDSKWQFWLQSGLEYFAMLGACFQDACLDCFPINFVVPLRAHIAN
S. montana Or42a2   SFQNYYPWLDWRASKWQFWLQSGLEYFAMLGACFQDACLDCFPINFVVPLRAHVAN
                   230       240       250       260       270       280
S. pallida Or42a2   FADRLRQLGNNPDEQPEQRYEKLIECIHDHKVILSFCDTLRPMIGGTIFVQLLVVG
S. flava Or42a3     LADRLRQLGNNPEEQPEQRYEKLIECIQDHKVILSFCDTLRPIIGGTIFVQLLVVG
S. flava Or42a4     LAERLREL GNNPEEQPEQRYEKLIECIQDHKVILSFCDILRPIIGGTIFVQLLIVG
S. montana Or42a2   LADRLRQLGNNPEEQPEQRYEKLIECIHDHKVILSFCDTLRPMIGGTIFVQLLIVG
                   290       300       310       320       330
S. pallida Or42a2   LVLGFTIINIVMFANFGSRIAAMSFMSAVLLETTPFCILCNYLADDCSKLADALFE
S. flava Or42a3     LLLGFTIINIVMFANFASRIAAMSYMSAVLLETTPFCILCNYLADDCNKLADALFE
S. flava Or42a4     LILGFTIINIVVFANFGSRIAAISYVPAVLLETTPFCILCNYLADDCNKLSDALFE
S. montana Or42a2   LLLGFTIINIVMFANFGSRIAAMSYMSAVLLETTPFCILCNYLANDCHKLADALFE
                   340       350       360       370       380       390
S. pallida Or42a2   SNWIDQEQRYKKTLLQFLQSLQKPIVFTAGNILTISVATNLNATKFSFSVFTLVKQ
S. flava Or42a3     SNWIDQEQRYKKTVLQFLQSLQKPIVFMAGNLFEISVATNLNATKFSFTVFTLVKQ
S. flava Or42a4     SNWIDQEQRYKKTVLQFLQSLQKPIVFMAGNLFEISVATNLNATKFSFTVFTFVKQ
S. montana Or42a2   SNWIDQEKRYKKTVLQFLQSLQKPIVFMAGNLFEISVATNLNATKFSFTVFTLVKQ
                   400       407
S. pallida Or42a2   MNIAEKLSKPSETE
S. flava Or42a3     MNIAEKLSKPSELIL
S. flava Or42a4     MNIAEKLSKPSE
S. montana Or42a2   MNIAEKLSKPSE
```

B

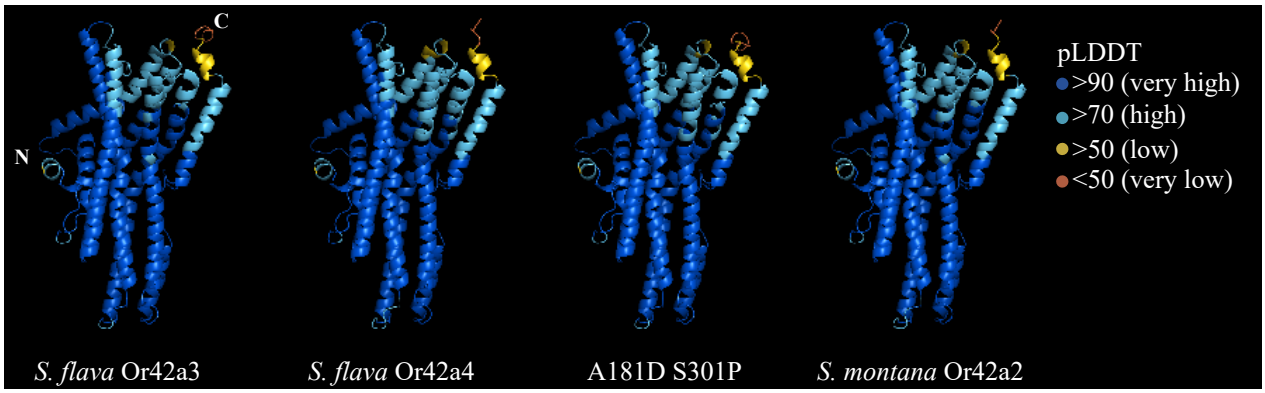

Supp. Figure 11

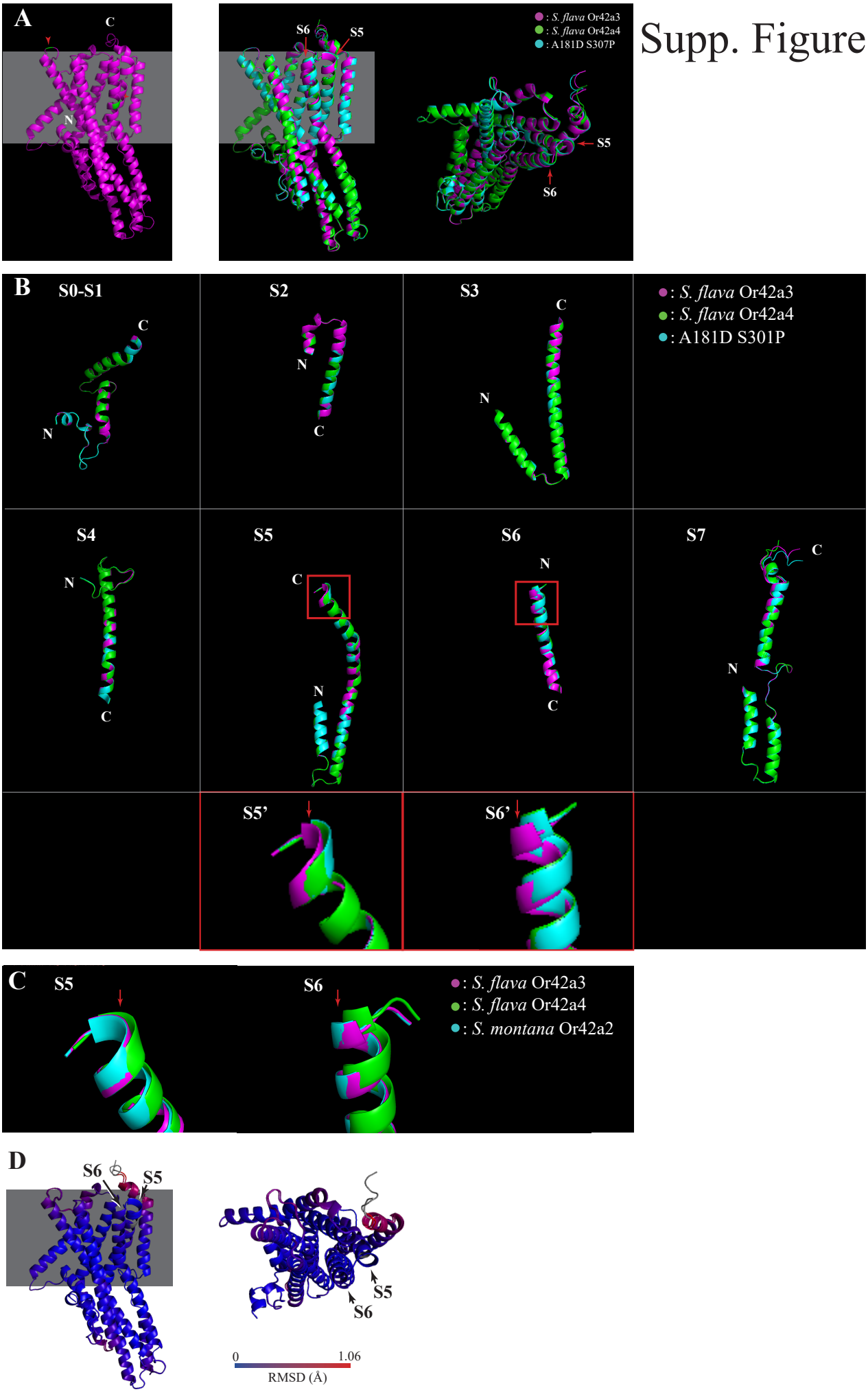

Supp. Figure 12

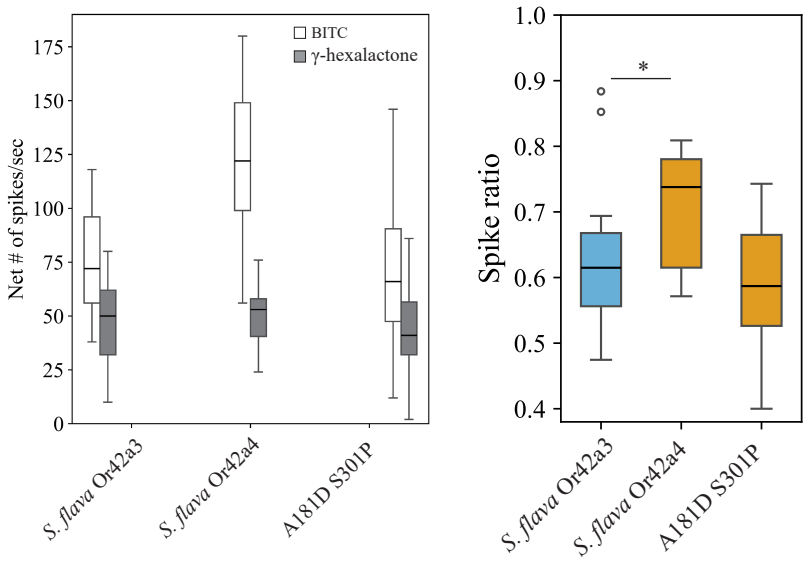
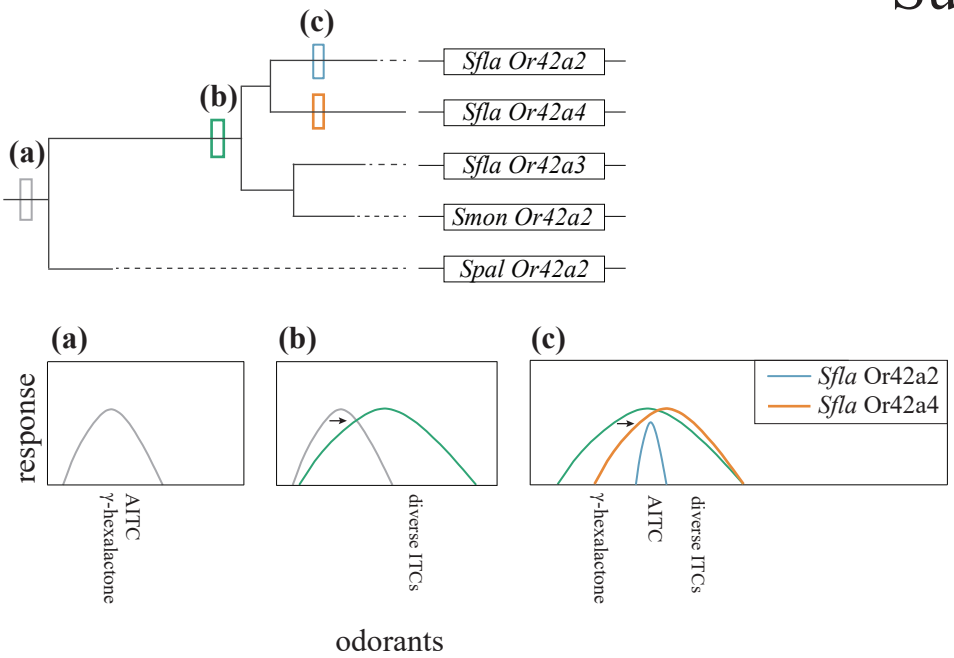
Supp. Figure 13